

Supplementary materials for

Synthesis of Novel 1-Oxo-2,3,4-trisubstituted Tetrahydroisoquinoline Derivatives, Bearing Other Heterocyclic Moieties and Comparative Preliminary Study of Anti-coronavirus Activity of Selected Compounds

Meglena I. Kandinska¹, Nikola T. Burdzhiev^{1,*}, Diana V. Cheshmedzhieva¹, Sonia V. Ilieva¹, Peter P. Grozdanov², Neli Vilhelmova-Ilieva², Nadya Nikolova², Vesela V. Lozanova³ and Ivanka Nikolova^{2,*}

Table of Contents

Spectra of <i>Rel</i> -(3R,4R)-3-(1 <i>H</i> -indol-3-yl)-2-(2-methoxyethyl)-1-oxo-1,2,3,4-tetrahydroisoquinoline-4-carboxylic acid (3)	2
Spectra of <i>Rel</i> -(3R,4R)-3-(1 <i>H</i> -indol-3-yl)- <i>N</i> -isopropyl- <i>N</i> -(isopropylcarbamoyl)-2-(2-methoxyethyl)-1-oxo-1,2,3,4-tetrahydroisoquinoline-4-carboxamide (4a).....	5
Spectra of <i>Rel</i> -(3R,4R)- <i>N</i> -isopropyl- <i>N</i> -(isopropylcarbamoyl)-2-(2-methoxyethyl)-1-oxo-3-(1-(piperidin-1-ylmethyl)-1 <i>H</i> -indol-3-yl)-1,2,3,4-tetrahydroisoquinoline-4-carboxamide (4b)	10
Spectra of <i>Rel</i> -(3R,4R)-3-(1 <i>H</i> -indol-3-yl)-2-(2-methoxyethyl)-4-(morpholine-4-carbonyl)-3,4-dihydroisoquinolin-1(2 <i>H</i>)-one (4c)	15
Spectra of <i>Rel</i> -(3R,4R)-4-(1 <i>H</i> -imidazole-1-carbonyl)-3-(1 <i>H</i> -indol-3-yl)-2-(2-methoxyethyl)-3,4-dihydroisoquinolin-1(2 <i>H</i>)-one (4d)	18
Spectra of <i>Rel</i> -(3R,4R)-3-(1 <i>H</i> -indol-3-yl)-2-(2-methoxyethyl)-4-(4-methylpiperazine-1-carbonyl)-3,4-dihydroisoquinolin-1(2 <i>H</i>)-one (4e).....	20
Spectra of <i>Rel</i> -(3R,4R)- and <i>rel</i> -(3 <i>S</i> ,4 <i>R</i>)-2-Hexyl-1-oxo-3-(pyridin-2-yl)-1,2,3,4-tetrahydroisoquinoline-4-carboxylic acids (<i>trans</i> - 6 and <i>cis</i> - 6).....	23
Spectra of <i>Rel</i> -(3R,4R)-2-Hexyl-4-(hydroxymethyl)-3-(pyridin-2-yl)-3,4-dihydroisoquinolin-1(2 <i>H</i>)-one (<i>trans</i> - 8)	24
Spectra of <i>Rel</i> -2-(((3 <i>S</i> ,4 <i>R</i>)-2-hexyl-1-oxo-3-(pyridin-2-yl)-1,2,3,4-tetrahydroisoquinolin-4-yl)methyl)isoindoline-1,3-dione (<i>trans</i> - 9)	26
Spectra of <i>Rel</i> -(3 <i>R</i> ,4 <i>S</i>)-4-(Aminomethyl)-2-hexyl-3-(pyridin-2-yl)-3,4-dihydroisoquinolin-1(2 <i>H</i>)-one (<i>trans</i> - 10)	28
Spectra of (<i>S</i>)- <i>N</i> -((3 <i>R</i> ,4 <i>S</i>)-2-hexyl-1-oxo-3-(pyridin-2-yl)-1,2,3,4-tetrahydroisoquinolin-4-yl)methyl)-3-phenyl-2-(2,2,2-trifluoroacetamido)propanamide and (<i>S</i>)- <i>N</i> -((3 <i>S</i> ,4 <i>R</i>)-2-hexyl-1-oxo-3-(pyridin-2-yl)-1,2,3,4-tetrahydroisoquinolin-4-yl)methyl)-3-phenyl-2-(2,2,2-trifluoroacetamido)propanamide (<i>trans</i> - 11a+trans-11b).....	29
Spectra of <i>Tert</i> -Butyl (<i>S</i>)-2-(((3 <i>R</i> ,4 <i>S</i>)-2-hexyl-1-oxo-3-(pyridin-2-yl)-1,2,3,4-tetrahydroisoquinolin-4-yl)methyl)carbamoyl)pyrrolidine-1-carboxylate and <i>tert</i> -butyl (<i>S</i>)-2-(((3 <i>S</i> ,4 <i>R</i>)-2-hexyl-1-oxo-3-(pyridin-	

2-yl)-1,2,3,4-tetrahydroisoquinolin-4-yl)methyl)carbamoyl)pyrrolidine-1-carboxylate (<i>trans</i> - 12a+<i>trans</i>-12b).....	31
(S)-N-((3 <i>R</i> ,4 <i>S</i>)-2-hexyl-1-oxo-3-(pyridin-2-yl)-1,2,3,4-tetrahydroisoquinolin-4-yl)methyl)-4-(methylthio)-2-(2,2,2-trifluoroacetamido)butanamide and (S)-N-((3 <i>S</i> ,4 <i>R</i>)-2-hexyl-1-oxo-3-(pyridin-2-yl)-1,2,3,4-tetrahydroisoquinolin-4-yl)methyl)-4-(methylthio)-2-(2,2,2-trifluoro-acetamido)butanamide (<i>trans</i> - 13a+<i>trans</i>-13b).....	33
Optimized geometry at PCM/M06-2X/6-31+G(d,p) level of theory (solvent dichloroethane) of trans-6a'	34

Spectra of *Rel*-(3*R*,4*R*)-3-(1*H*-indol-3-yl)-2-(2-methoxyethyl)-1-oxo-1,2,3,4-tetrahydroisoquinoline-4-carboxylic acid (3**)**

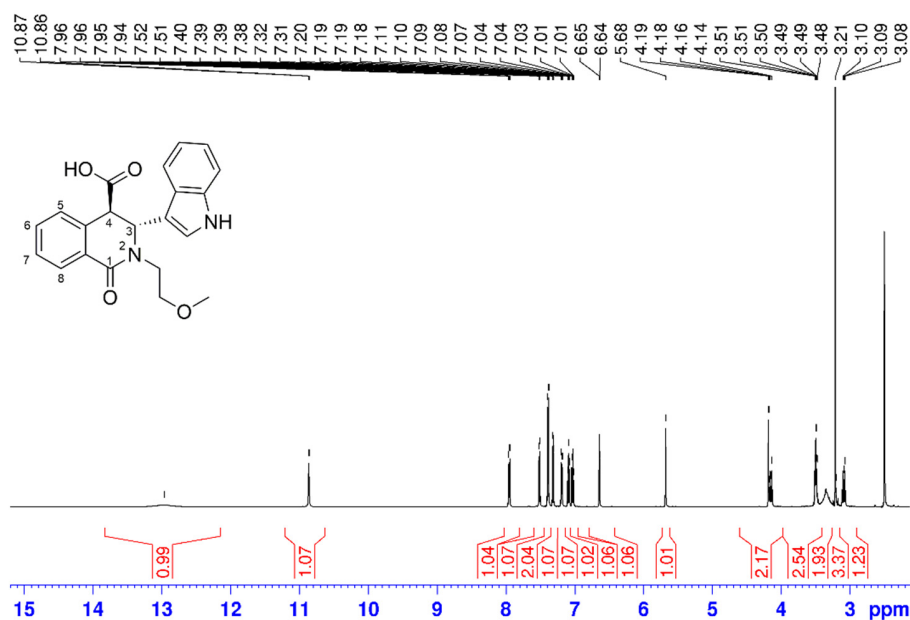


Figure S1. ¹H NMR (DMSO-*d*₆) of acid *trans*-**3** at 298 K.

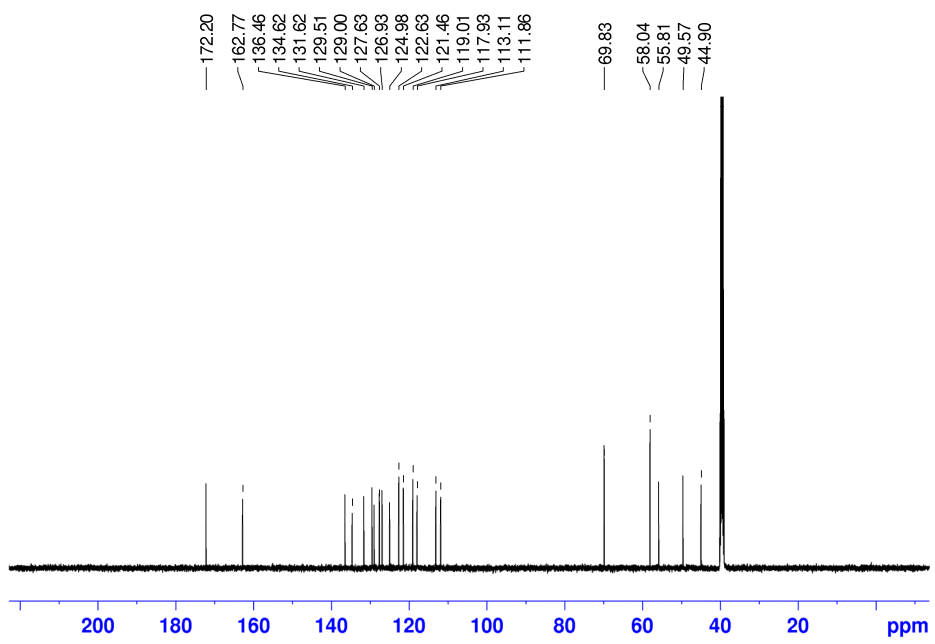
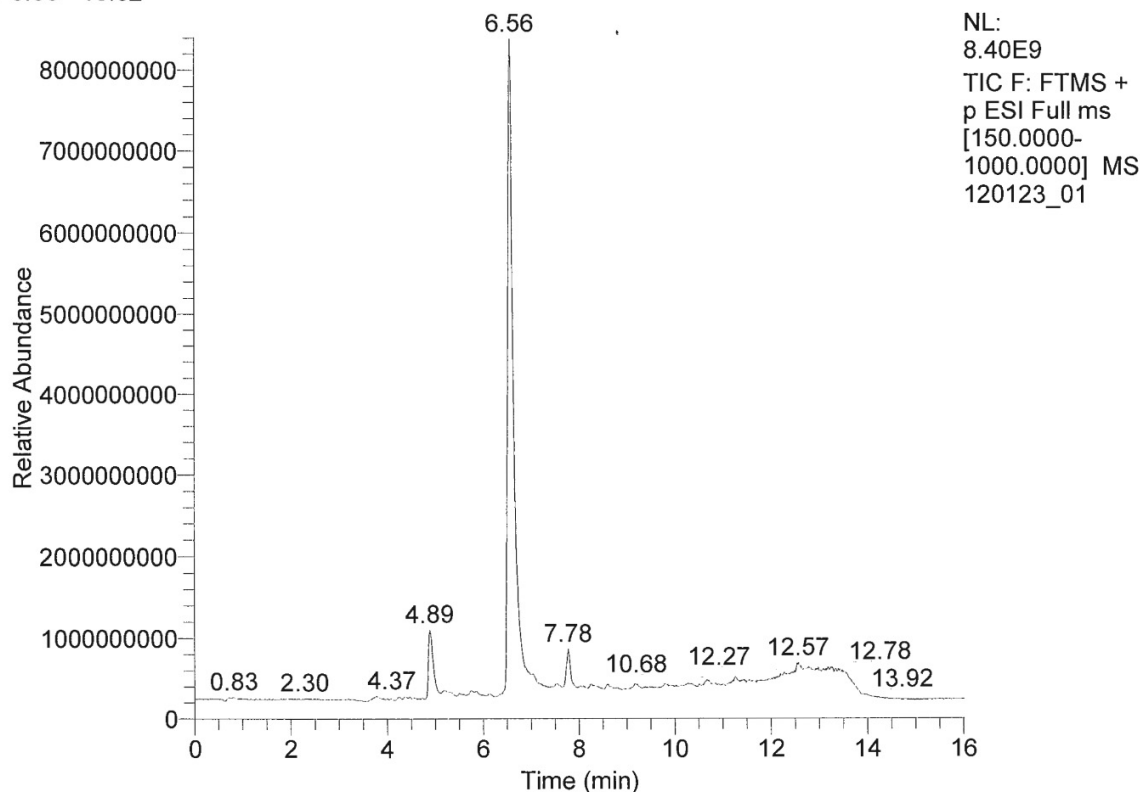


Figure S2. ¹³C NMR (*DMSO-d*₆) of acid *trans*-3 at 298 K.

RT: 0.00 - 16.02



120123_01 #490-496 RT: 6.55-6.63 AV: 7 NL: 3.08E9
T: FTMS + p ESI Full ms [150.0000-1000.0000]

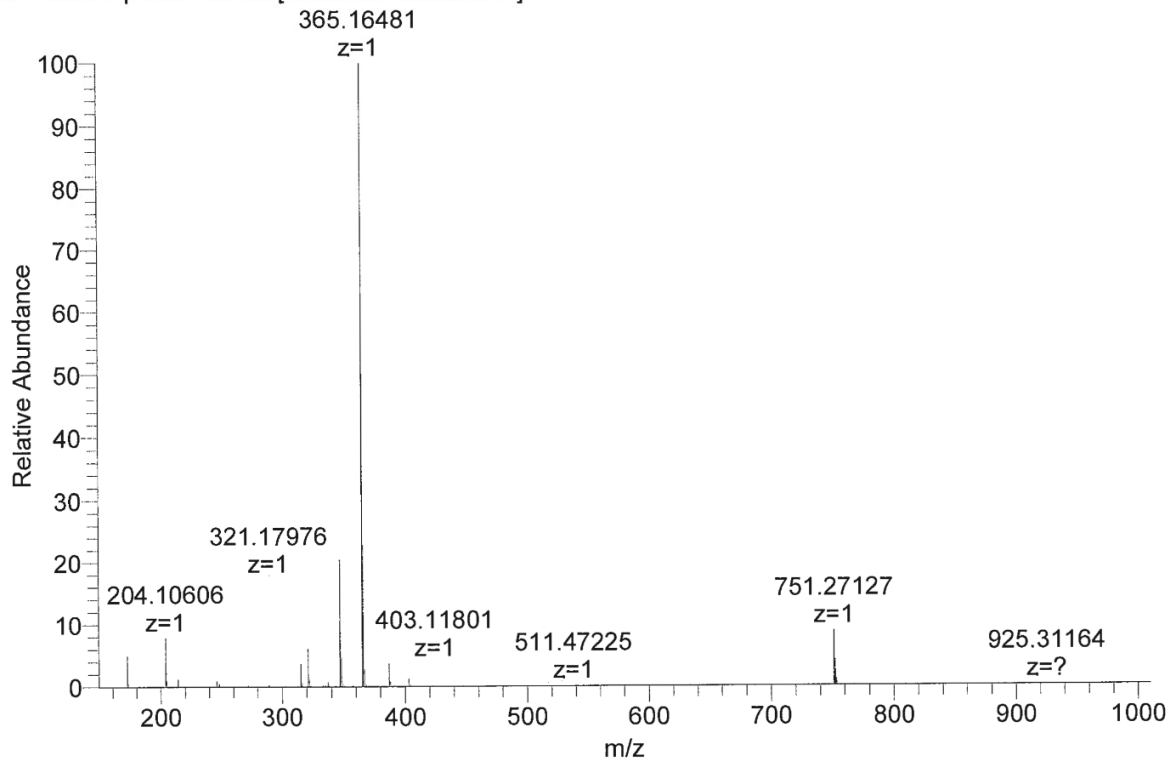


Figure S3. HRMS spectrum of acid *trans*-3.

Spectra of *Rel*-(3R,4R)-3-(1*H*-indol-3-yl)-*N*-isopropyl-*N*-(isopropylcarbamoyl)-2-(2-methoxyethyl)-1-oxo-1,2,3,4-tetrahydroisoquinoline-4-carboxamide (**4a**)

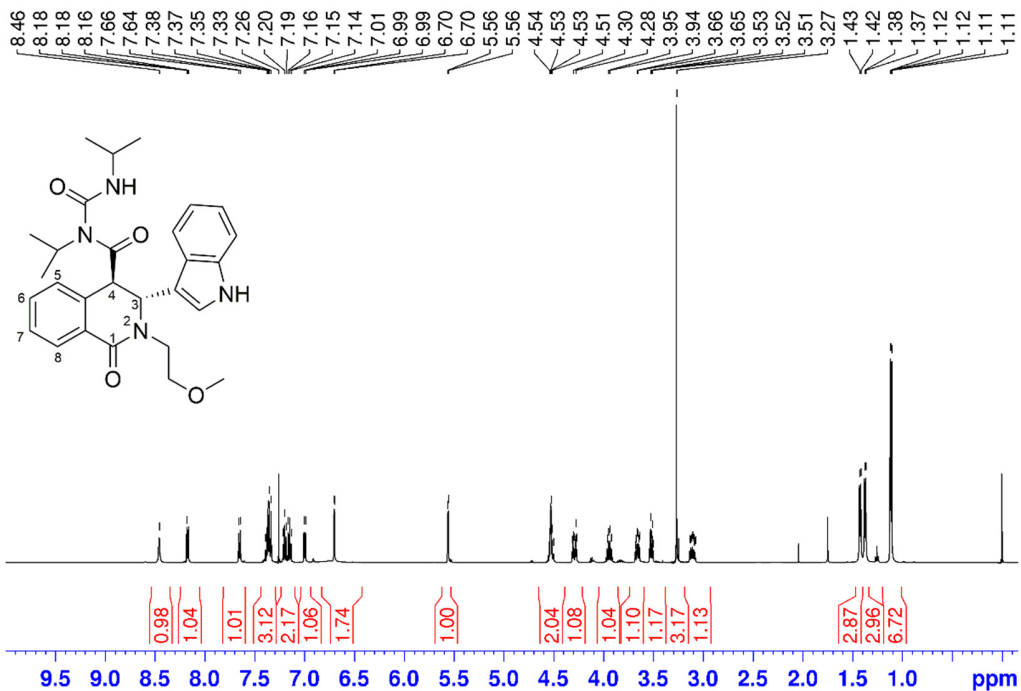


Figure S4. ^1H NMR (CDCl_3) of **4a** at 298 K.

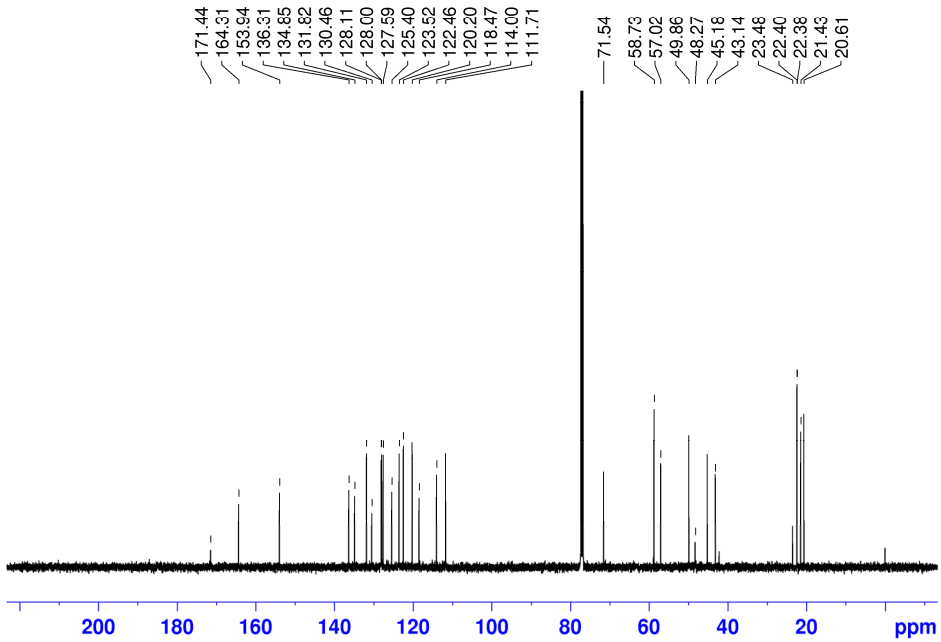


Figure S5. ^{13}C NMR (CDCl_3) of **4a** at 298 K.

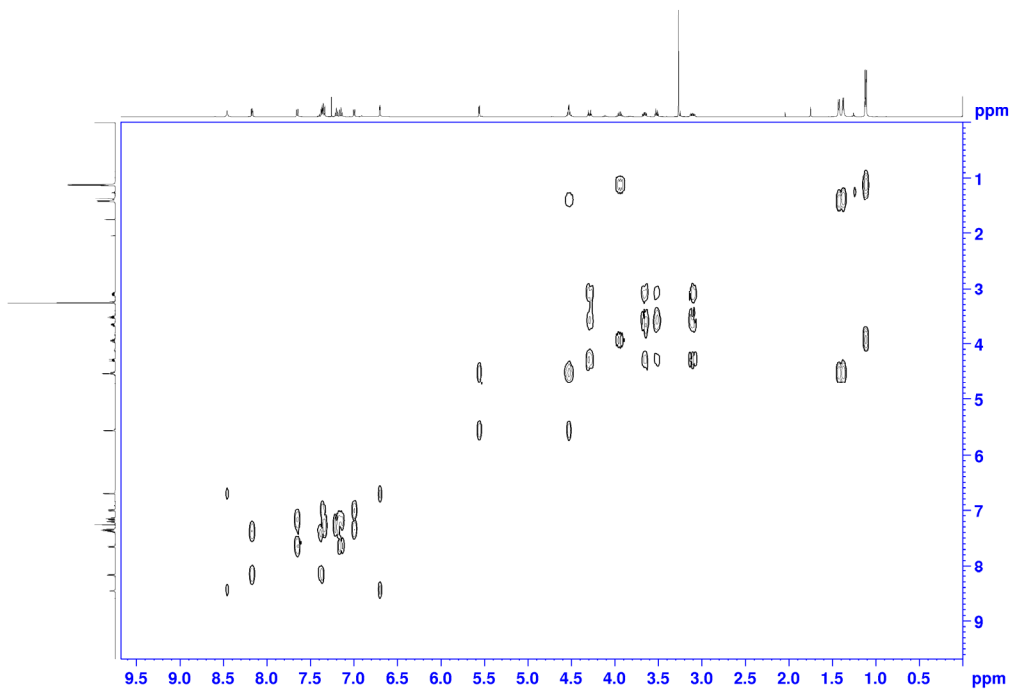


Figure S6. COSY NMR (CDCl_3) of **4a** at 298 K.

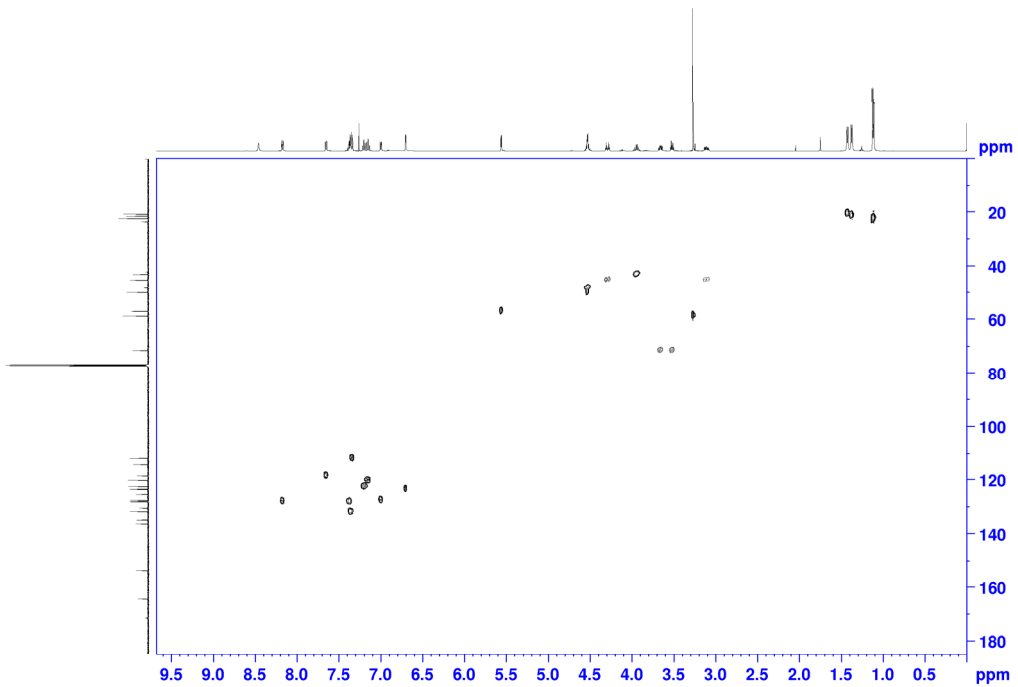


Figure S7. HSQC NMR (CDCl_3) of **4a** at 298 K.

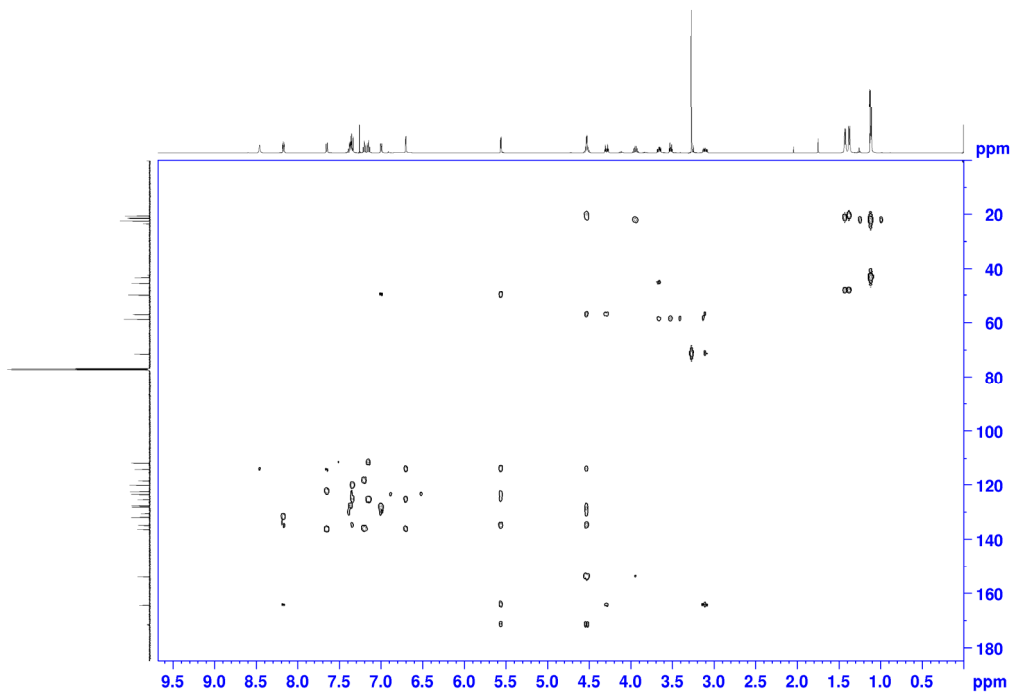


Figure S8. HMBC NMR (CDCl_3) of **4a** at 298 K.

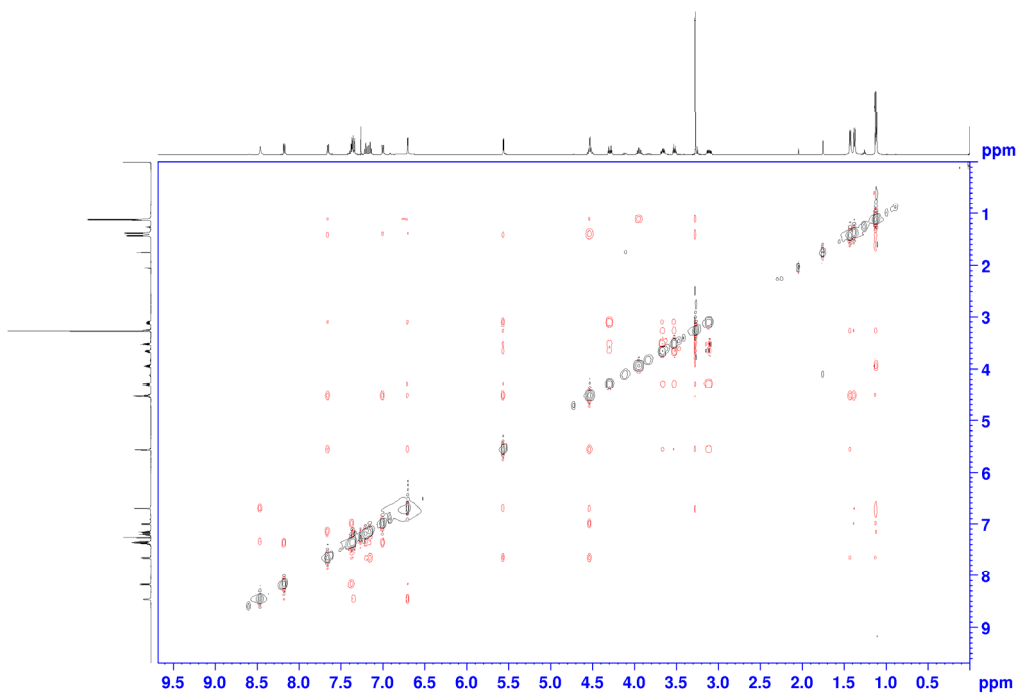
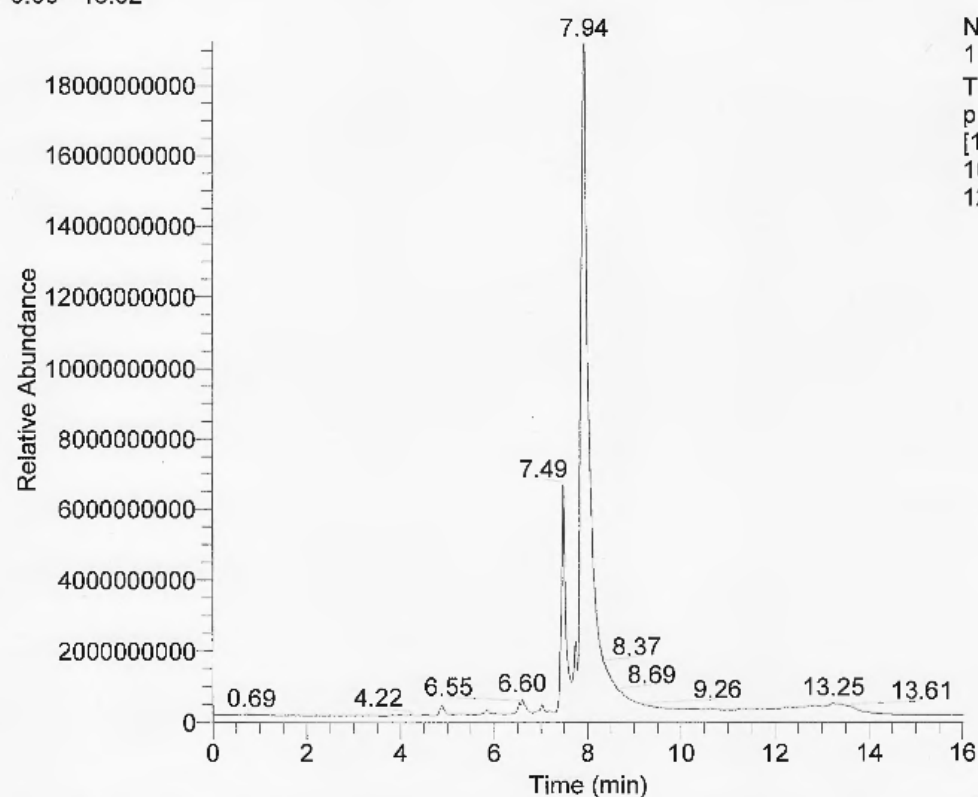


Figure S9. NOESY NMR (CDCl_3) of **4a** at 298 K.

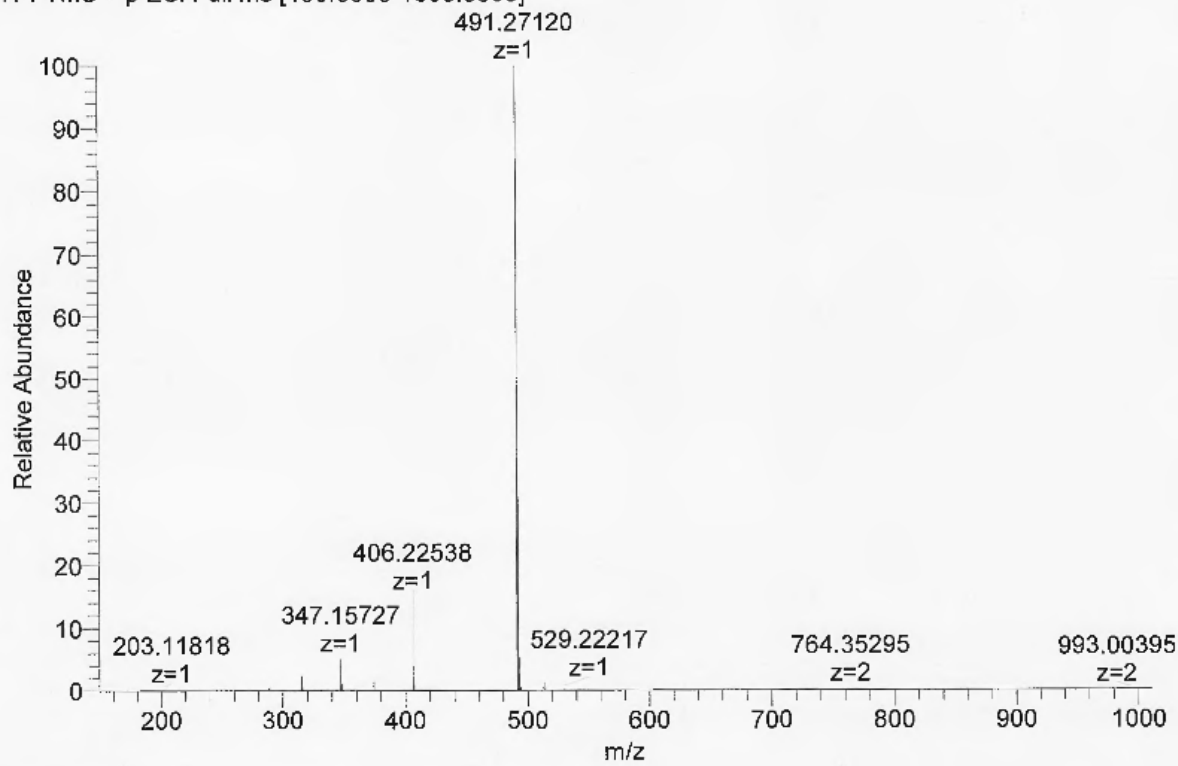
RT: 0.00 - 16.02



NL:
1.93E10
TIC F: FTMS +
p ESI Full ms
[150.0000-
1000.0000] MS
120123_07

120123_07 #590-596 RT: 7.89-7.97 AV: 7 NL: 9.77E9

T: FTMS + p ESI Full ms [150.0000-1000.0000]

Figure S10. HRMS spectrum of **4a**.

Spectra of *Rel*-(3R,4R)-N-isopropyl-N-(isopropylcarbamoyl)-2-(2-methoxyethyl)-1-oxo-3-(1-piperidin-1-ylmethyl)-1*H*-indol-3-yl)-1,2,3,4-tetrahydroisoquinoline-4-carboxamide (**4b**)

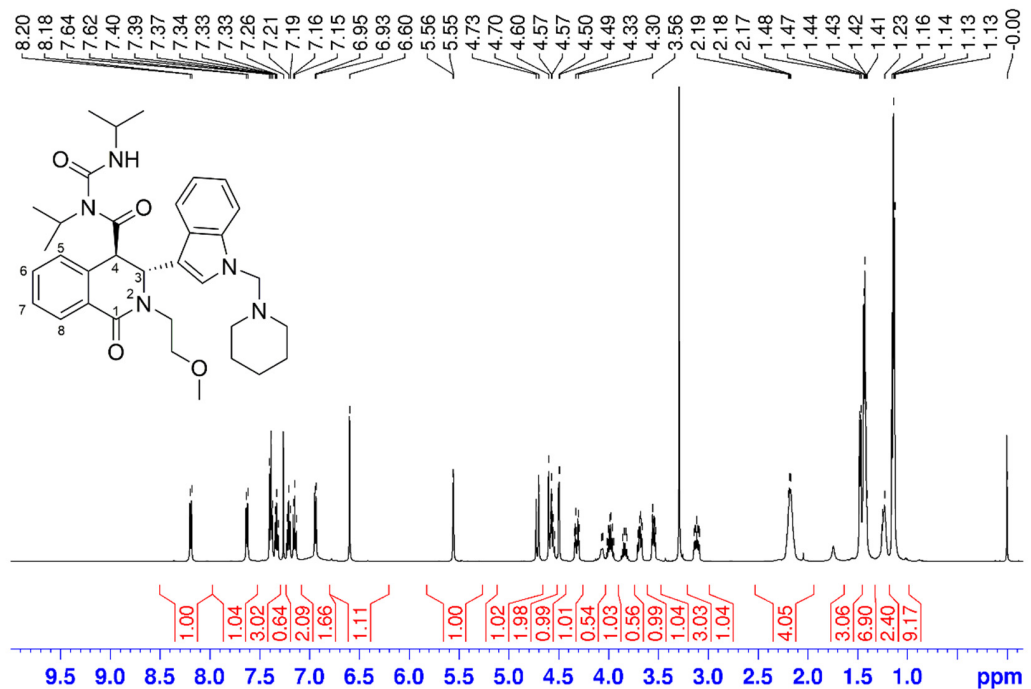


Figure S11. ^1H NMR (CDCl_3) of **4b** at 298 K.

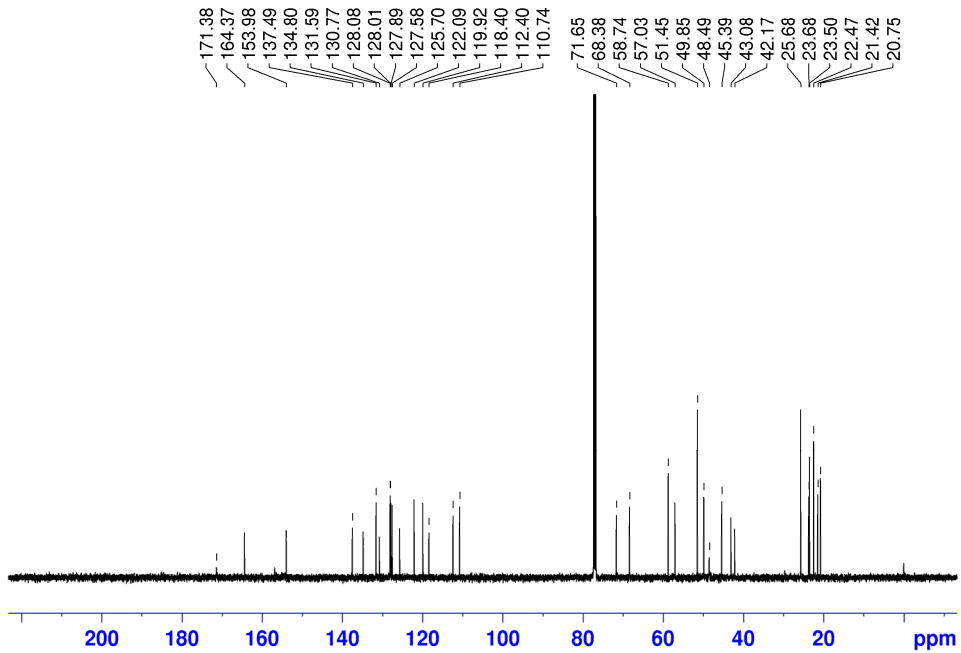


Figure S12. ^{13}C NMR (CDCl_3) of **4b** at 298 K.

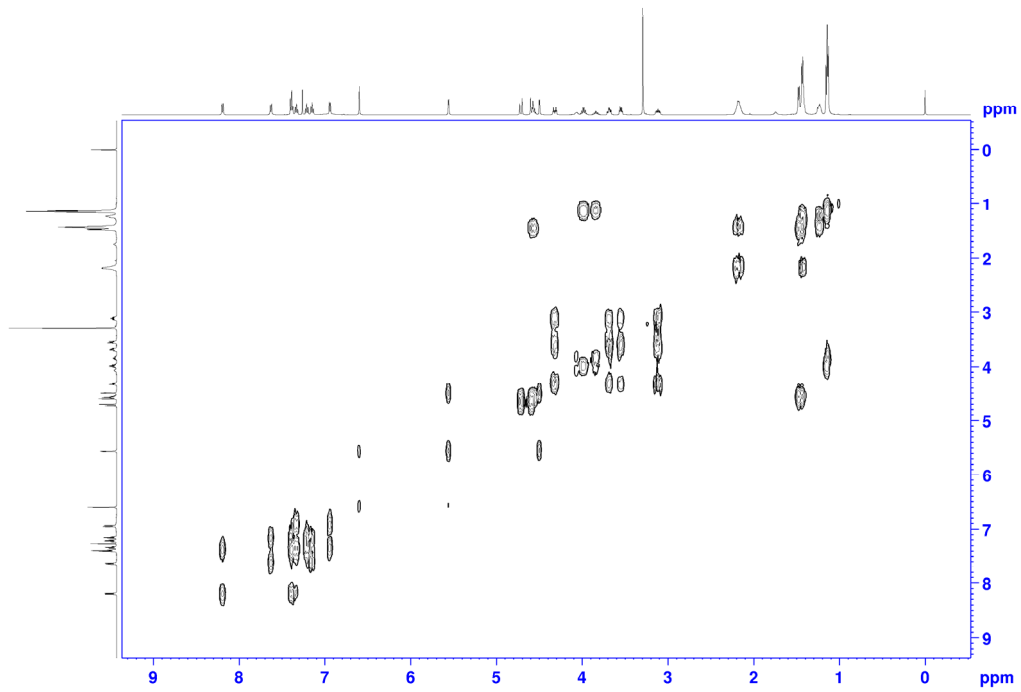


Figure S13. COSY NMR (CDCl_3) of **4b** at 298 K.

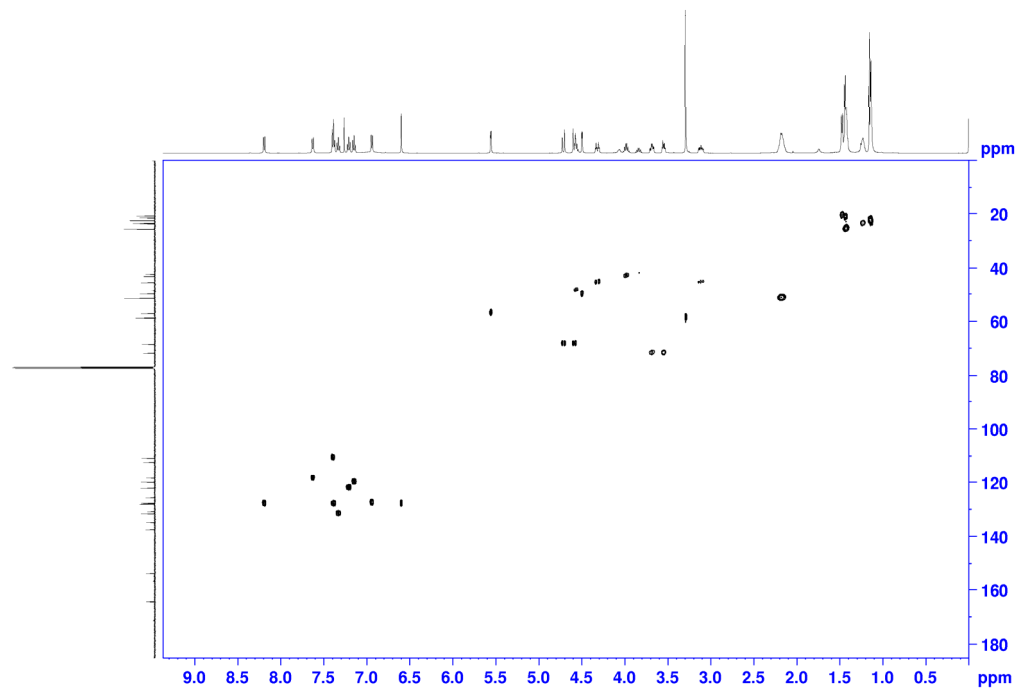


Figure S14. HSQC NMR (CDCl_3) of **4b** at 298 K.

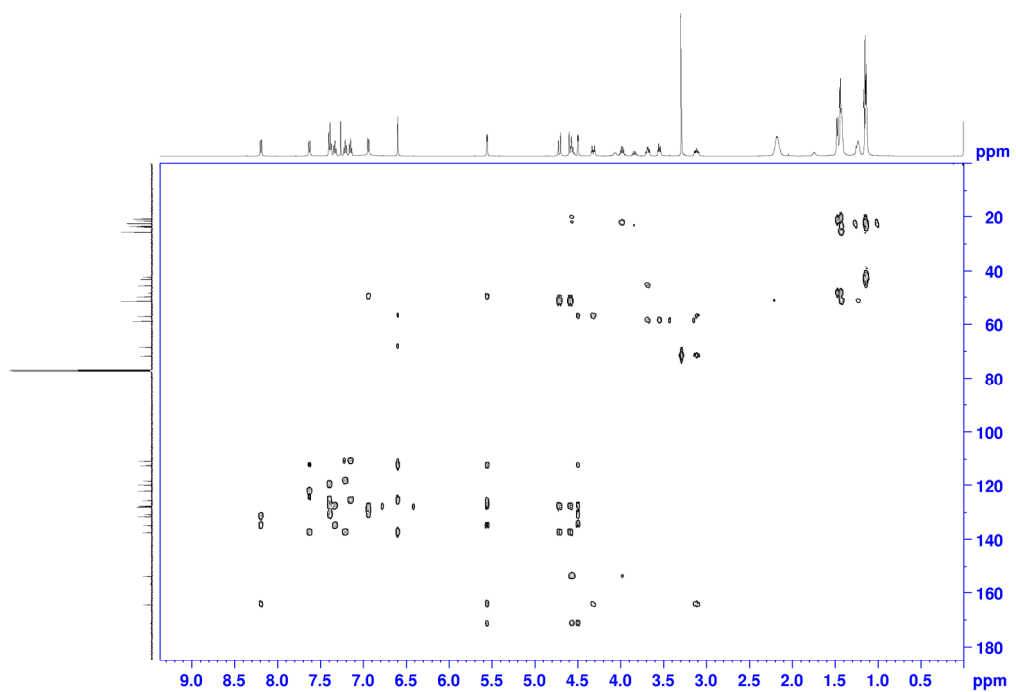


Figure S15. HMBC NMR (CDCl_3) of **4b** at 298 K.

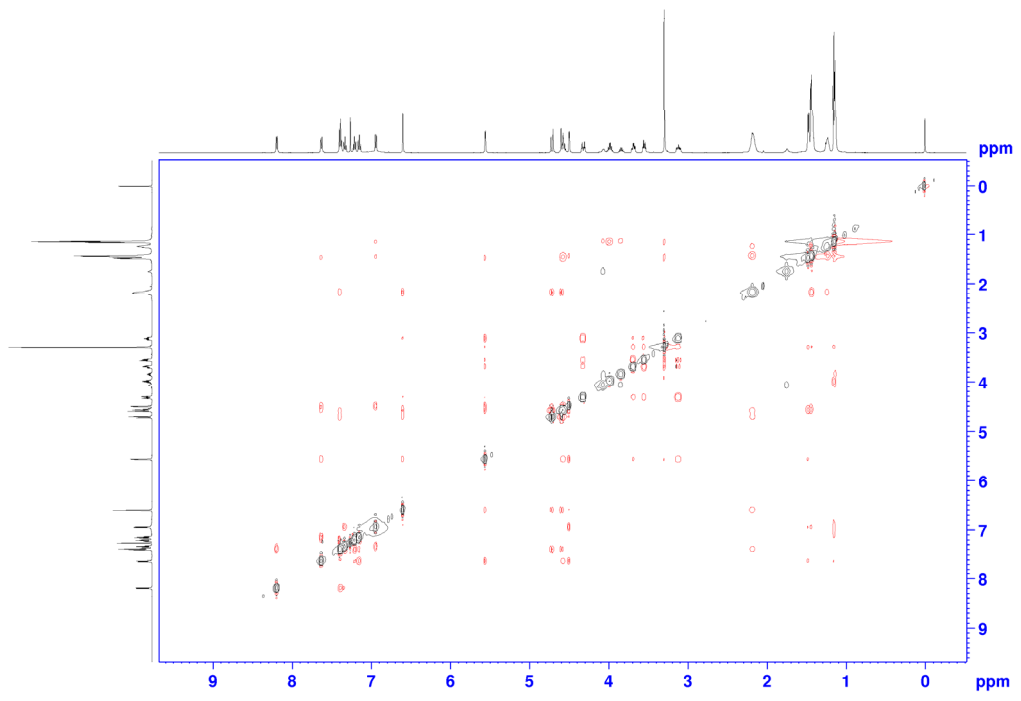
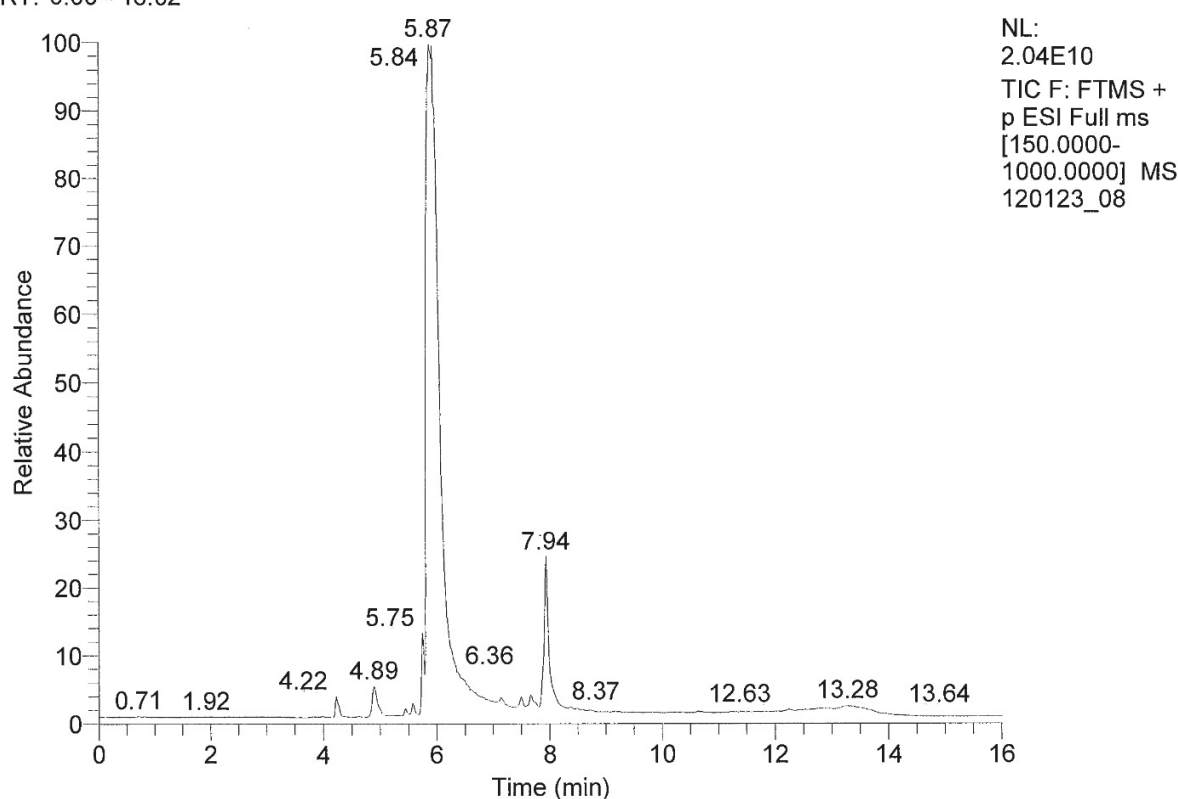


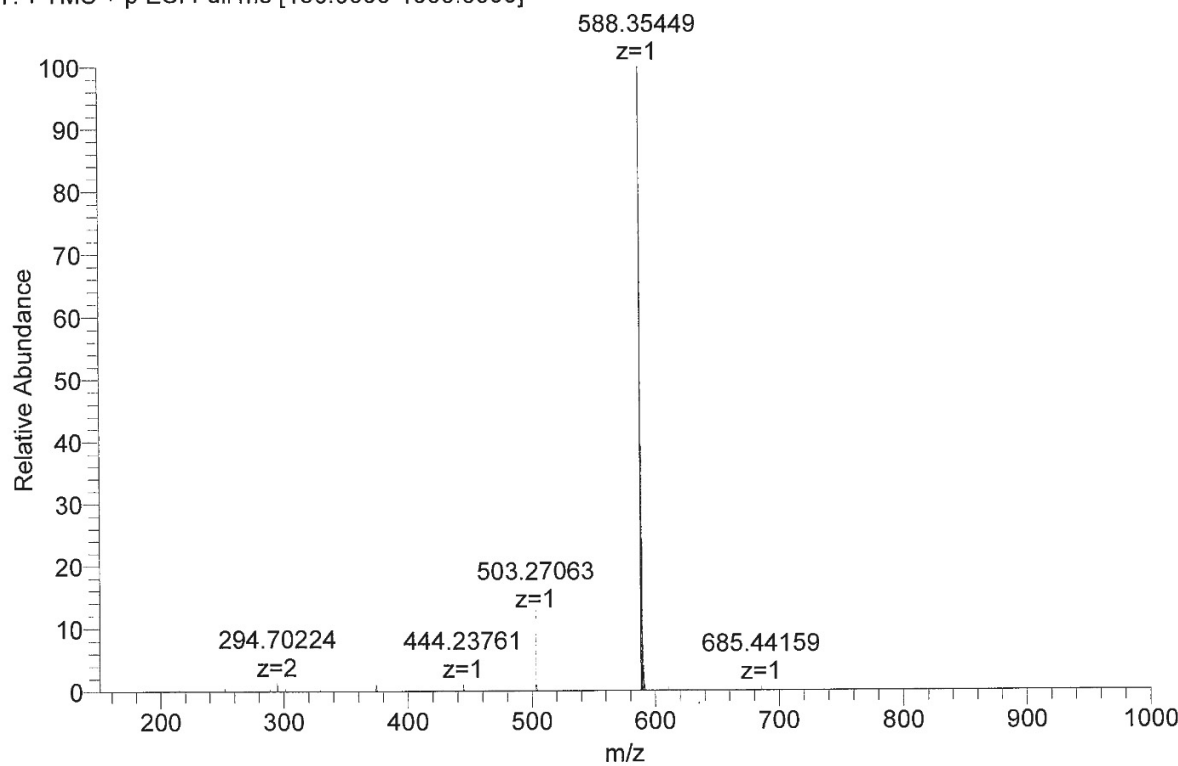
Figure S16. NOESY NMR (CDCl_3) of **4b** at 298 K.

RT: 0.00 - 16.02



120123_08 #442 RT: 5.91 AV: 1 NL: 1.12E10

T: FTMS + p ESI Full ms [150.0000-1000.0000]

Figure S17. HRMS spectrum of **4b**.

Spectra of *Rel*-(3*R*,4*R*)-3-(1*H*-indol-3-yl)-2-(2-methoxyethyl)-4-(morpholine-4-carbonyl)-3,4-dihydroisoquinolin-1(2*H*)-one (**4c**)

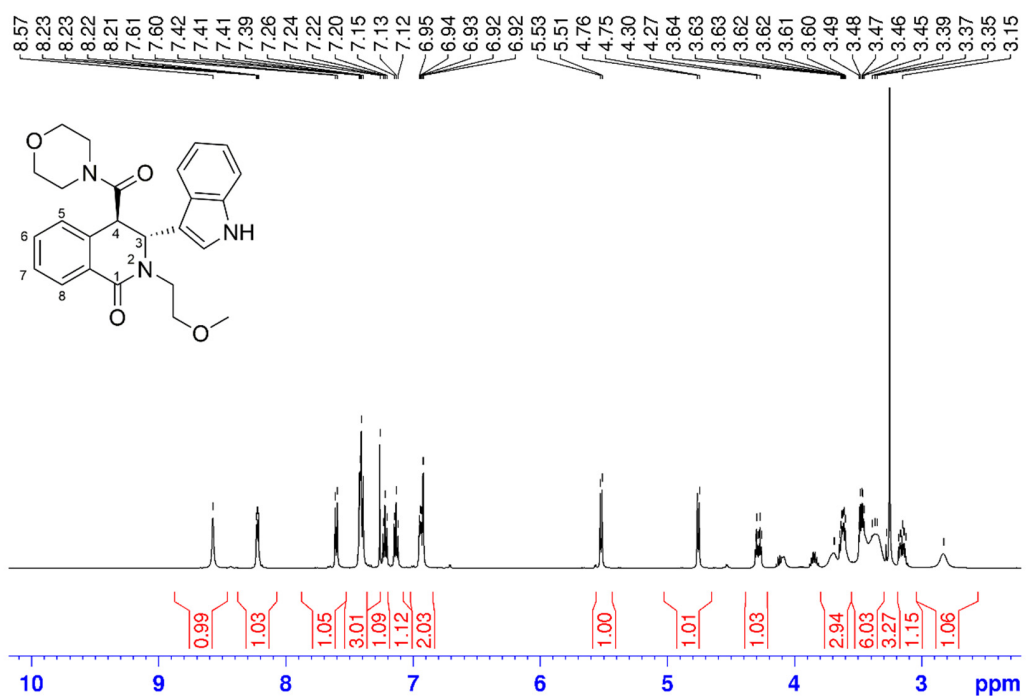


Figure S18. ^1H NMR (CDCl_3) of **4c** at 298 K.

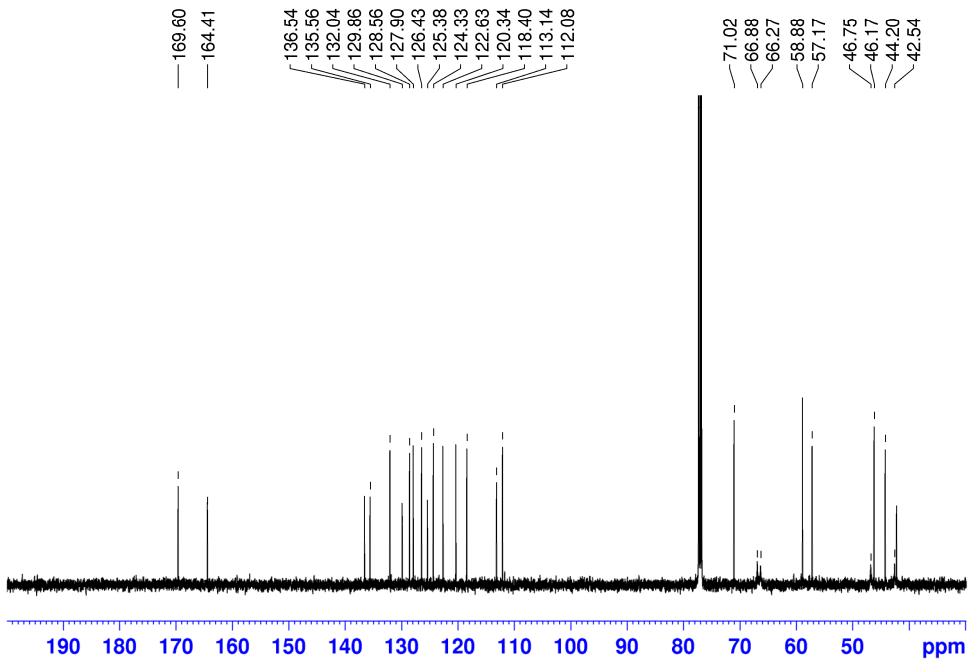
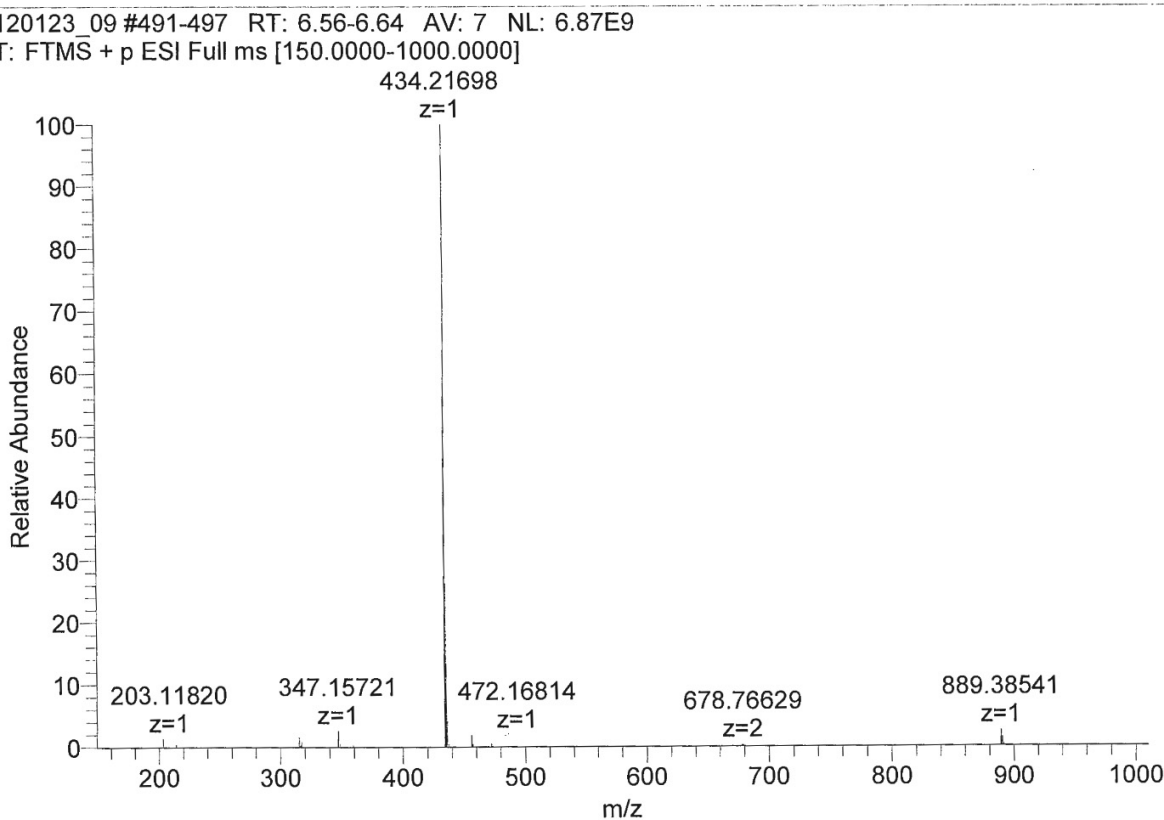
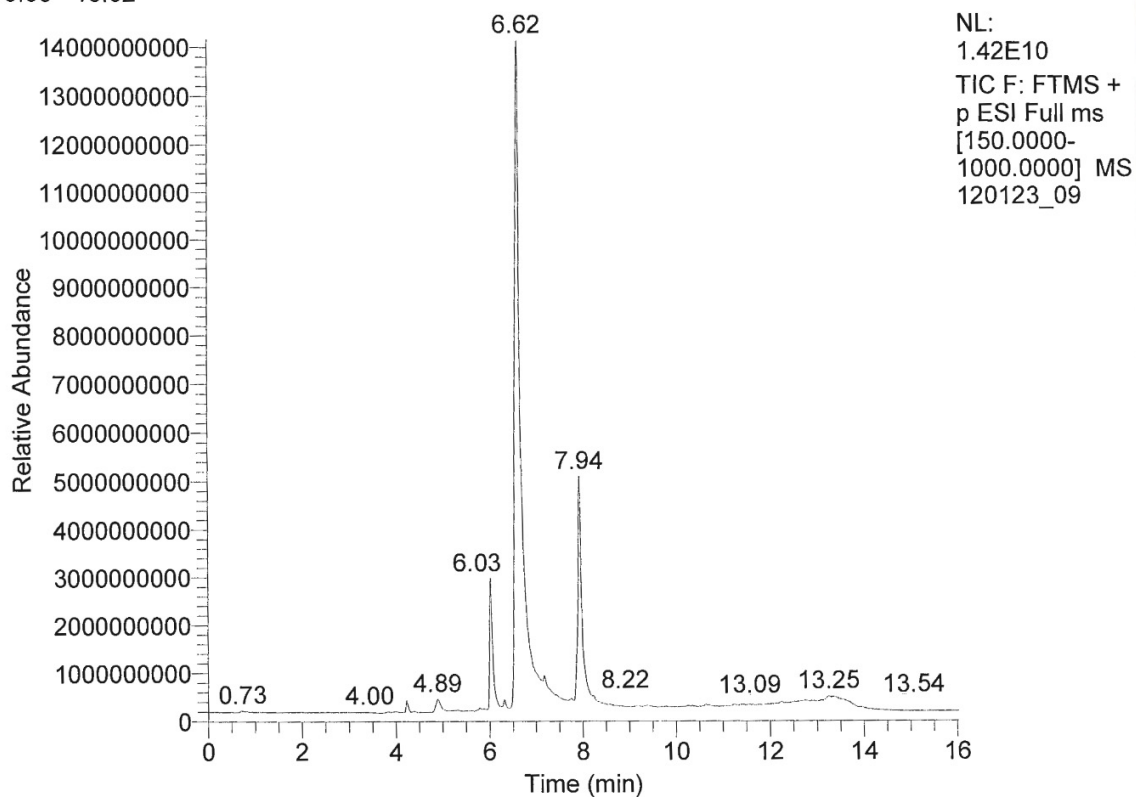


Figure S19. ^{13}C NMR NMR (CDCl_3) of **4c** at 298 K.

RT: 0.00 - 16.02

Figure S20. HRMS spectrum of **4c**.

Spectra of *Rel*-(3*R*,4*R*)-4-(1*H*-imidazole-1-carbonyl)-3-(1*H*-indol-3-yl)-2-(2-methoxyethyl)-3,4-dihydroisoquinolin-1(2*H*)-one (**4d**)

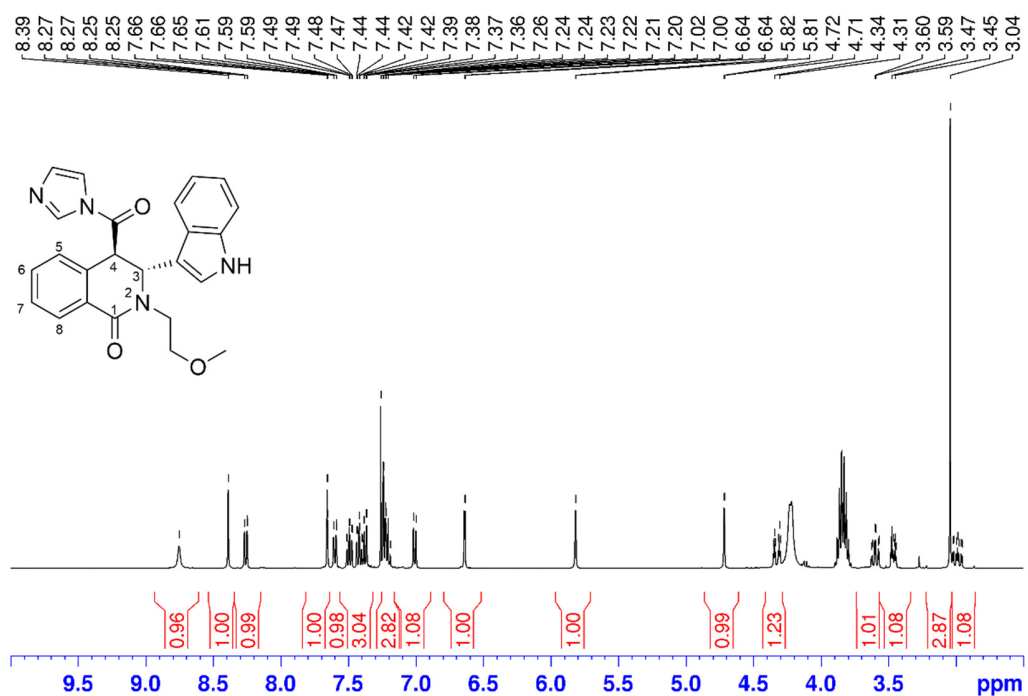


Figure S21. ¹H NMR (400.23 MHz, CDCl₃) of **4d** at 298 K.

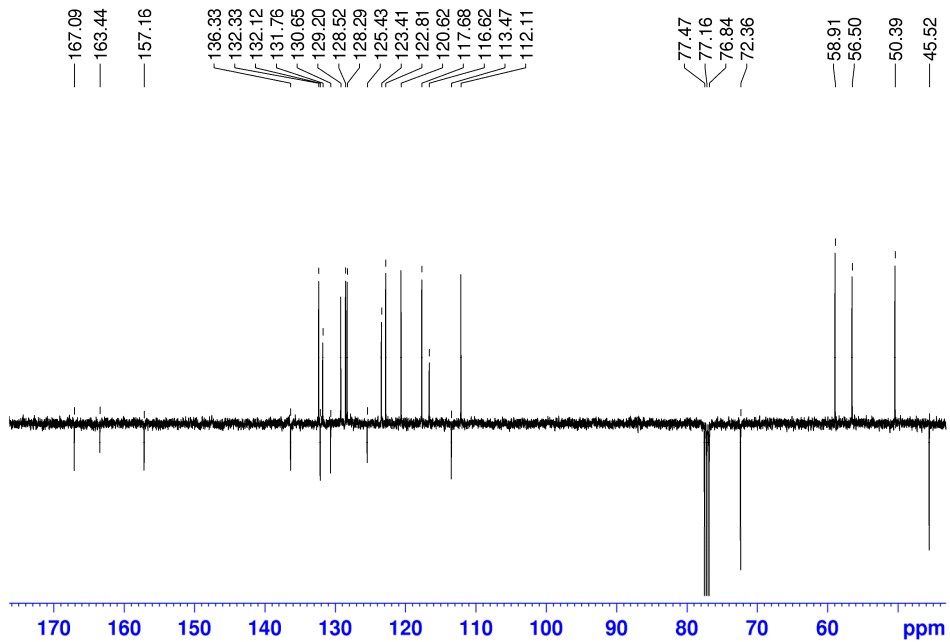


Figure S22. ¹³C NMR using J-modulated spin-echo (100.64 MHz, CDCl₃) of **4d** at 298 K.

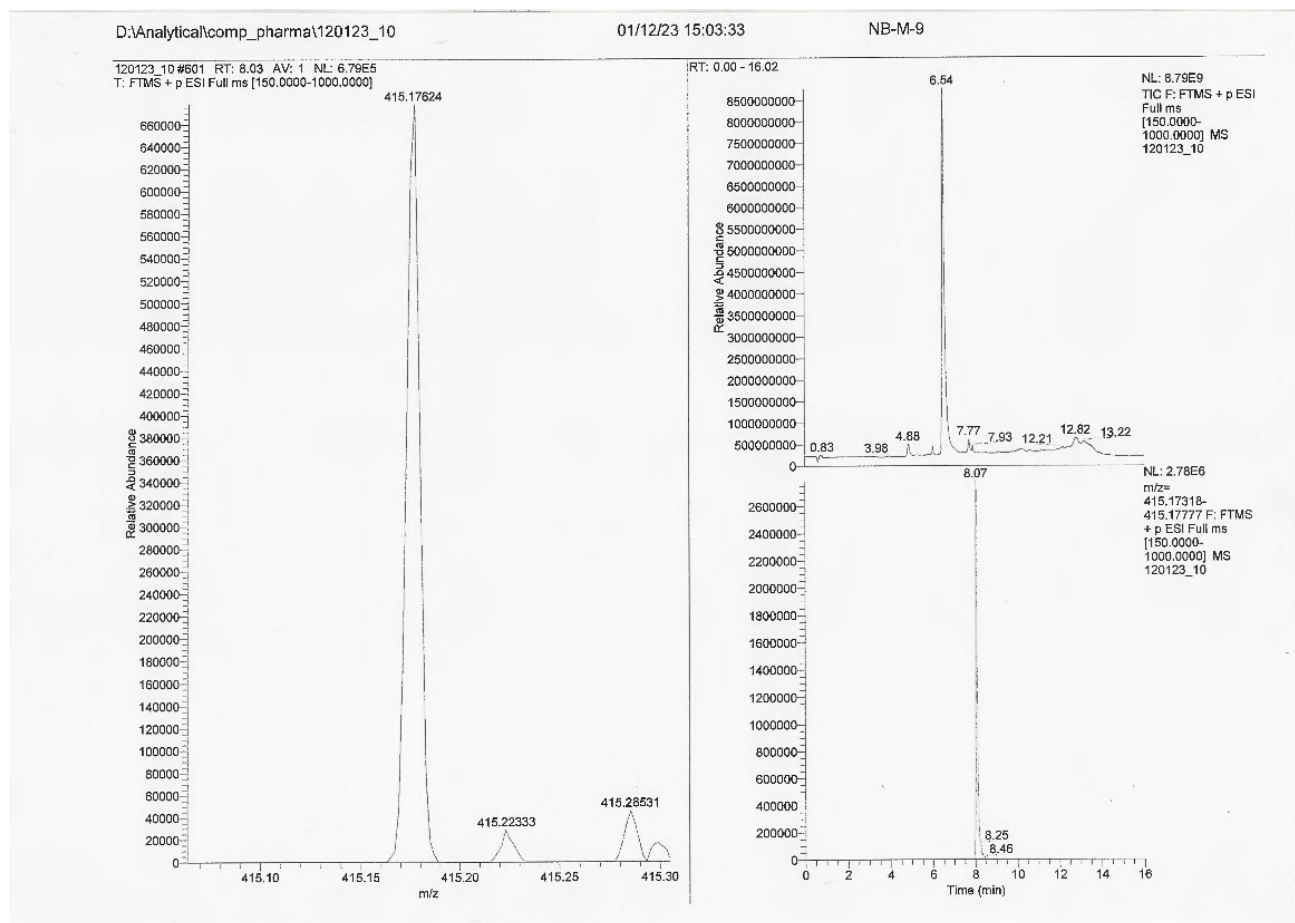


Figure S23. HRMS spectrum of **4d**.

Spectra of *Rel*-(3*R*,4*R*)-3-(1*H*-indol-3-yl)-2-(2-methoxyethyl)-4-(4-methylpiperazine-1-carbonyl)-3,4-dihydroisoquinolin-1(2*H*)-one (**4e**)

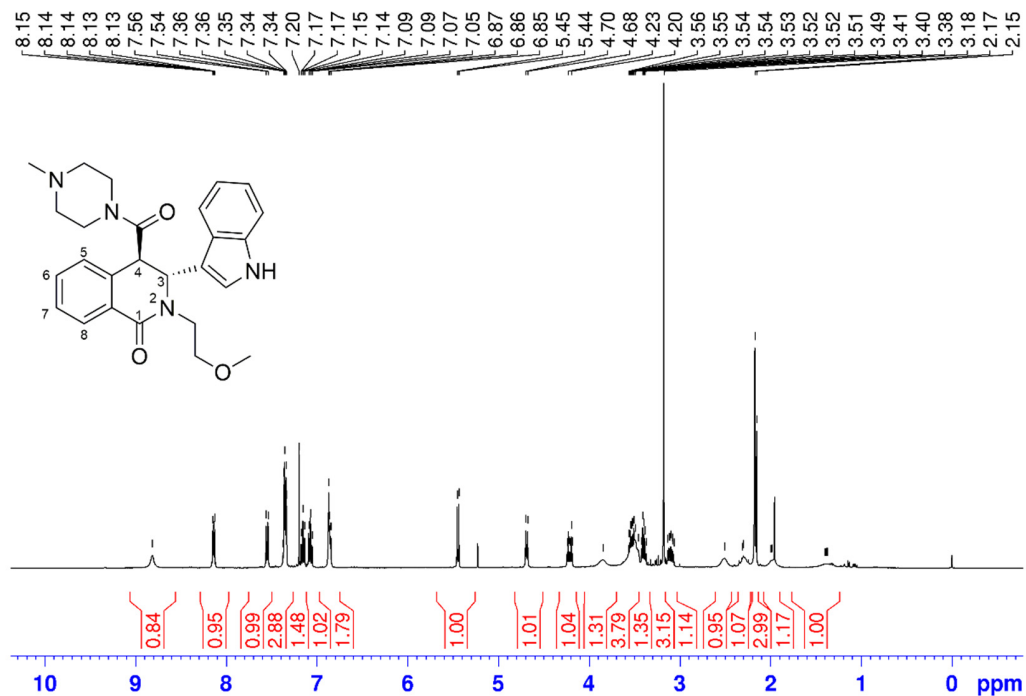


Figure S24. ¹H NMR (400.23 MHz, CDCl₃) of **4e** at 298 K.

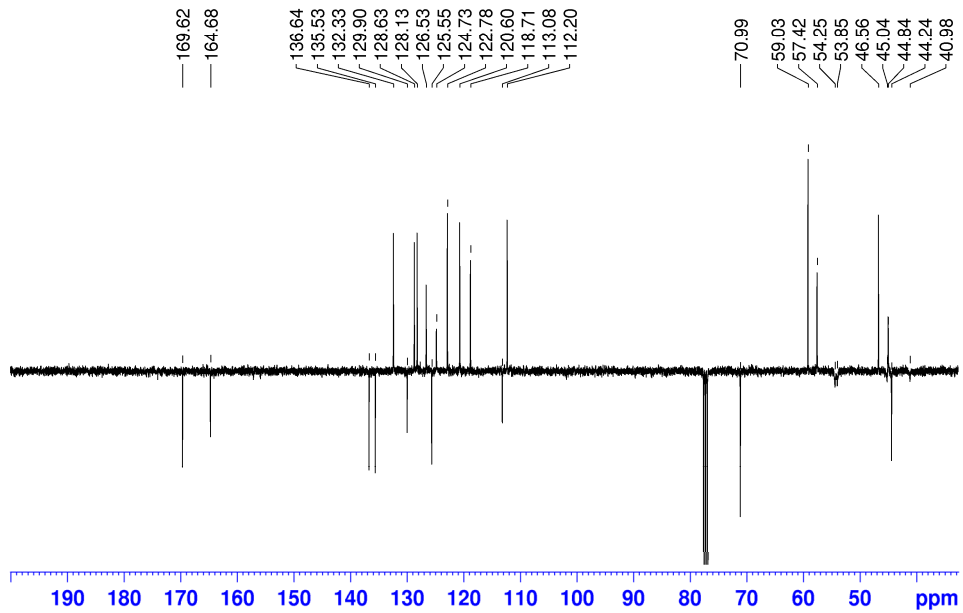
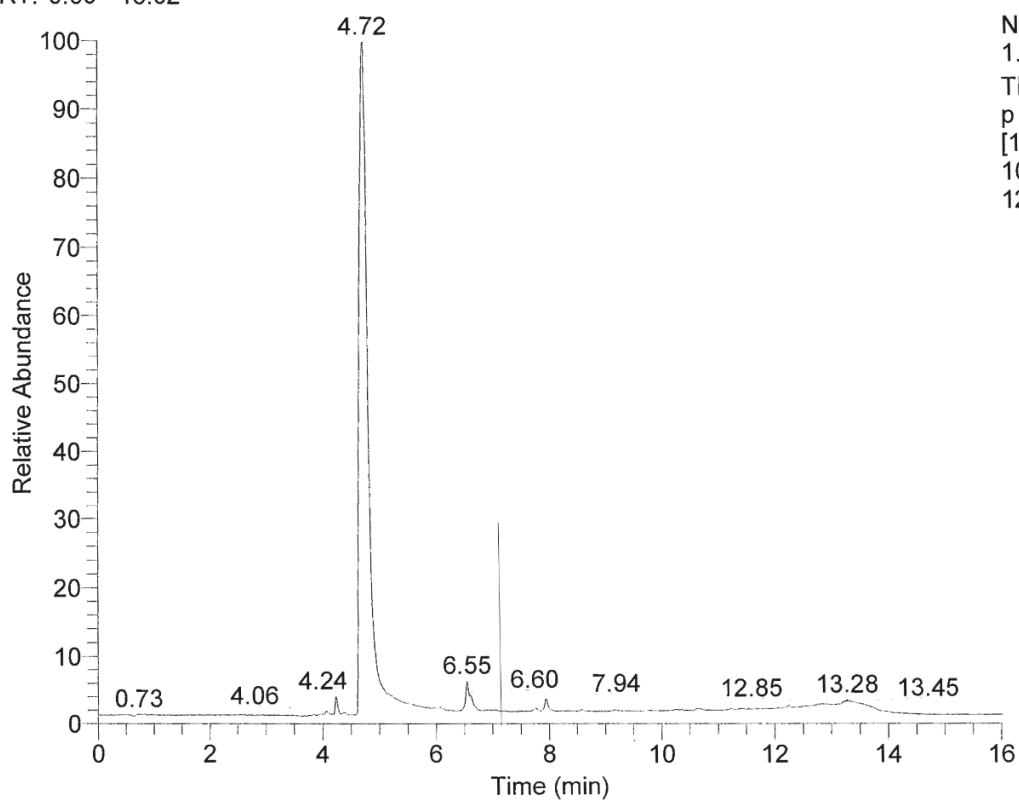


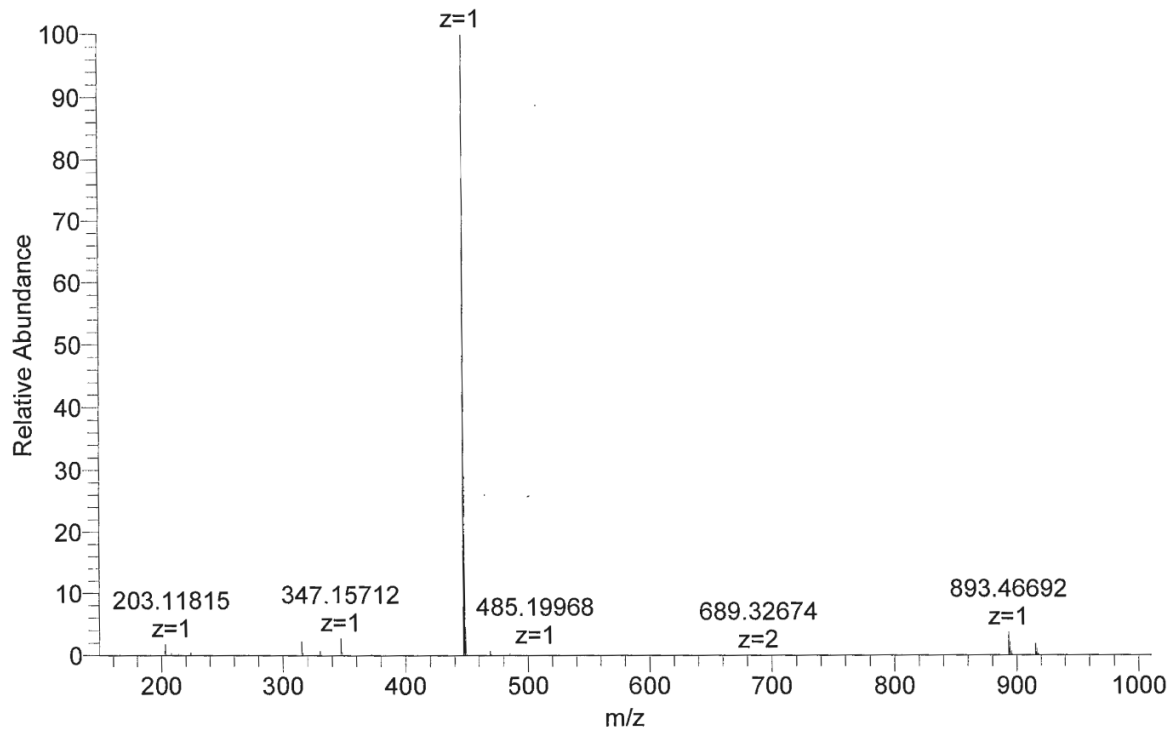
Figure S25. ^{13}C NMR using J-modulated spin-echo (100.64 MHz, CDCl_3) of **4e** at 298 K.

RT: 0.00 - 16.02



120123_11 #350-357 RT: 4.68-4.77 AV: 8 NL: 7.64E9
T: FTMS + p ESI Full ms [150.0000-1000.0000]

447.24884

Figure S26. HRMS spectrum of **4e**.

Spectra of *Rel*-(3*R*,4*R*)- and *rel*-(3*S*,4*R*)-2-Hexyl-1-oxo-3-(pyridin-2-yl)-1,2,3,4-tetrahydroisoquinoline-4-carboxylic acids (*trans*-6 and *cis*-6)

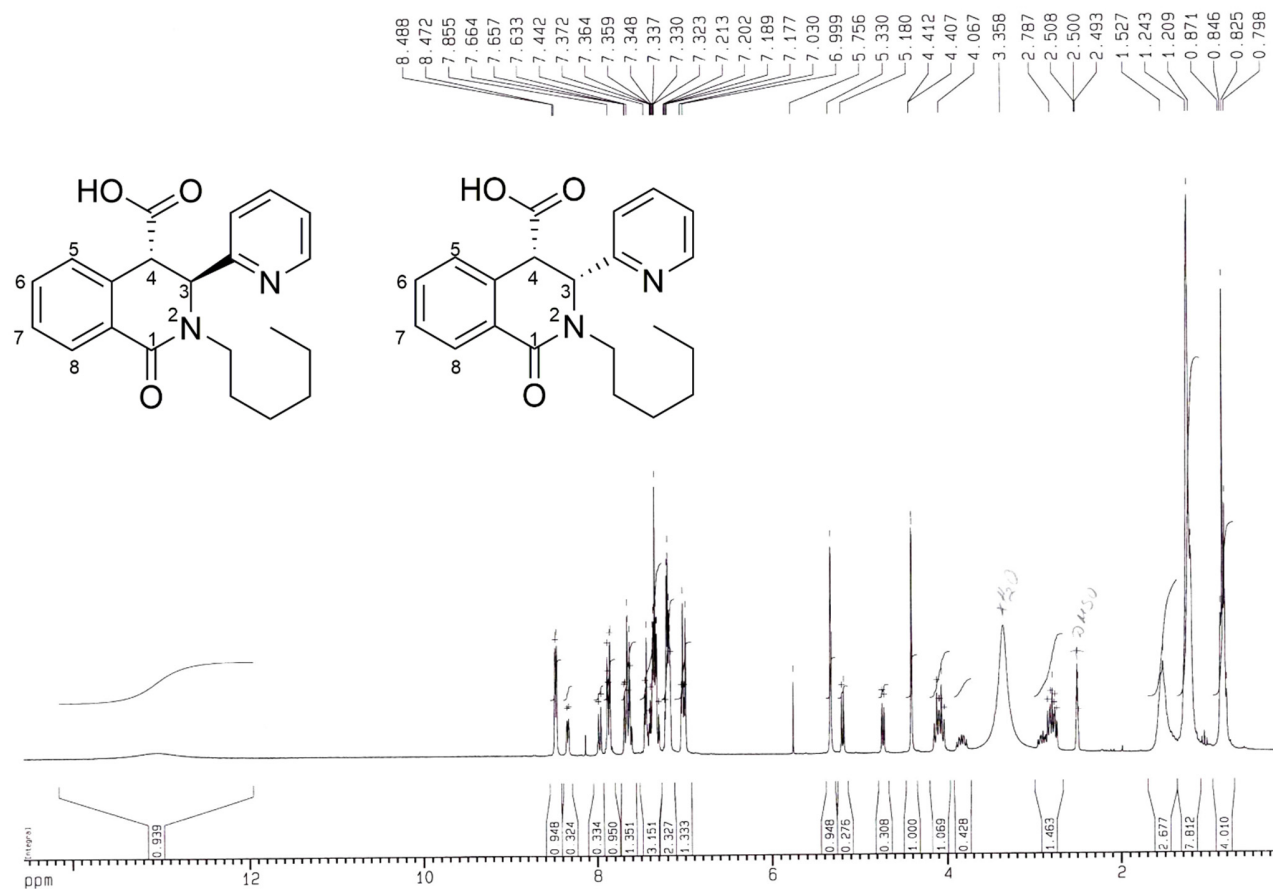


Figure S27. ¹H NMR (DMSO-d₆) of *trans*-6 and *cis*-6 at 298 K.

Spectra of *Rel*-(3*R*,4*R*)-2-Hexyl-4-(hydroxymethyl)-3-(pyridin-2-yl)-3,4-dihydroisoquinolin-1(2*H*)-one (*trans*-8)

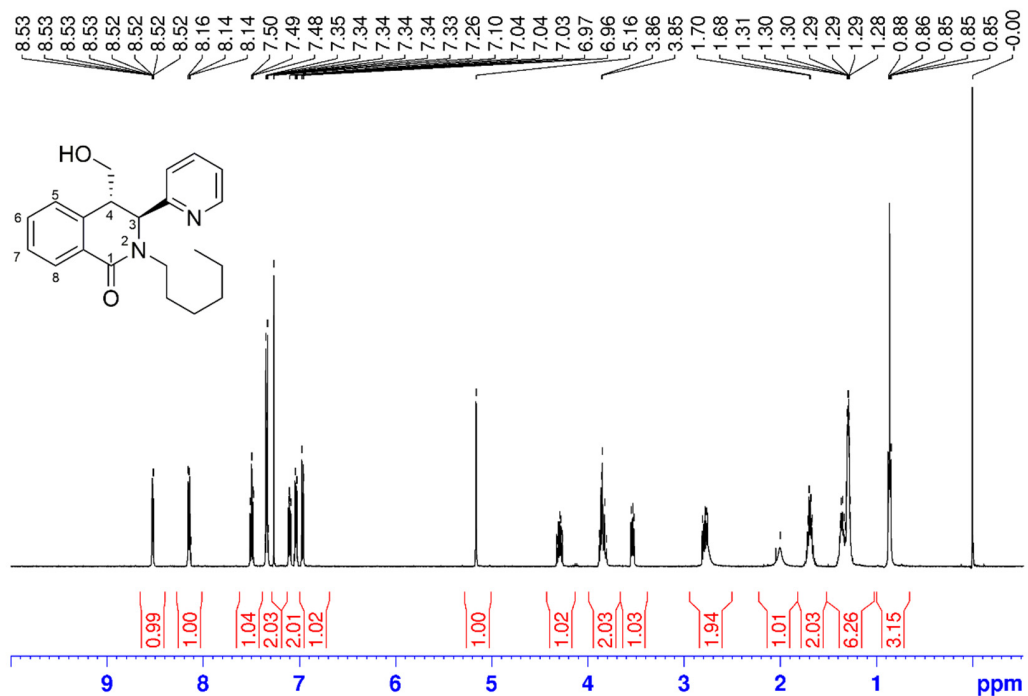


Figure S28. ¹H NMR (500.13 MHz, CDCl₃) of *trans*-8 at 298 K.

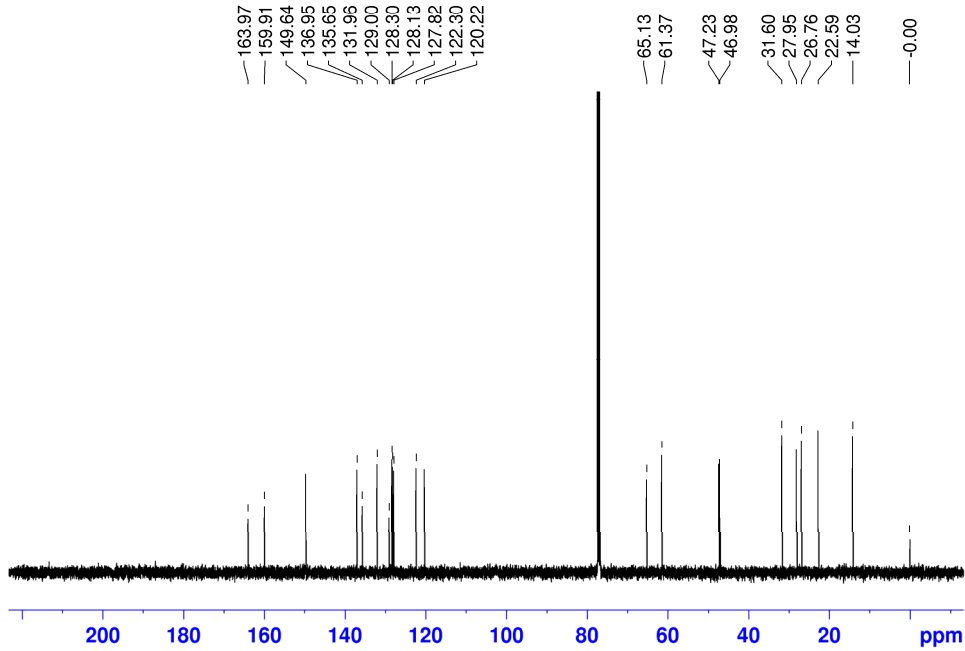


Figure S29. ^{13}C NMR (CDCl_3) of *trans*-8 at 298 K.

Spectra of *Rel*-2-(((3*S*,4*R*)-2-hexyl-1-oxo-3-(pyridin-2-yl)-1,2,3,4-tetrahydroisoquinolin-4-yl)methyl)isoindoline-1,3-dione (*trans*-9)

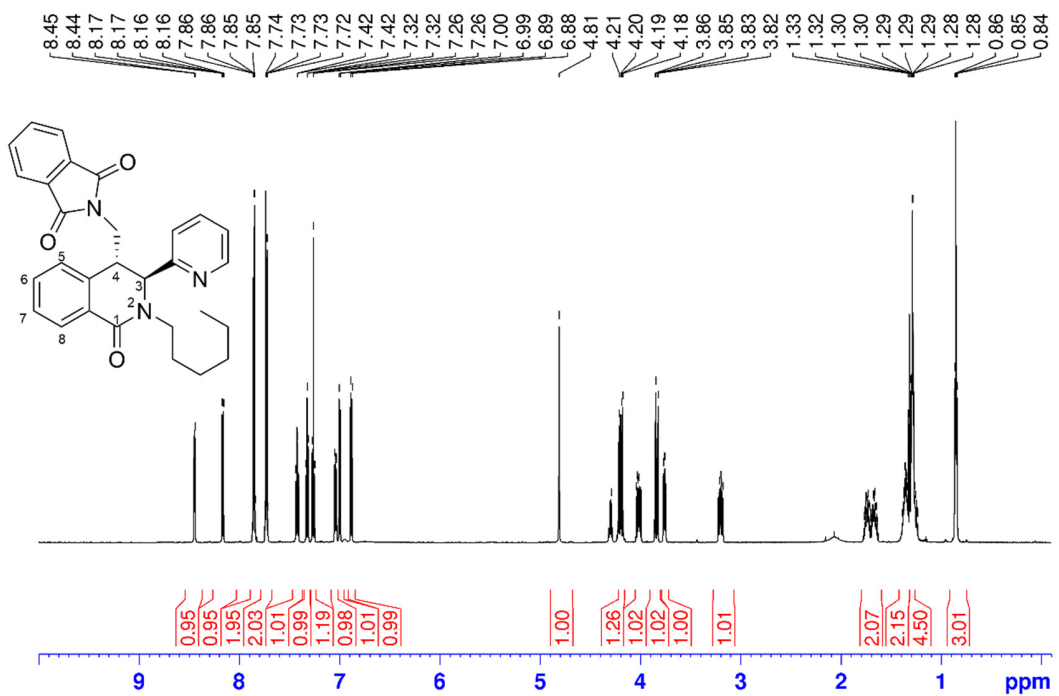


Figure S30. ^1H NMR (600.18 MHz, CDCl_3) of *trans*-9 at 298 K.

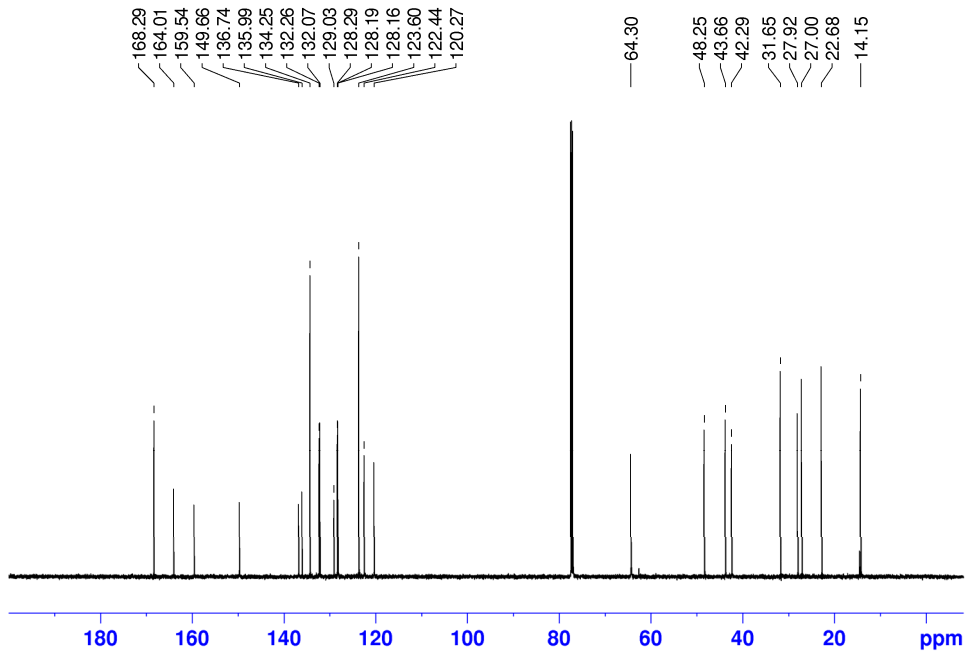


Figure S31. ^{13}C NMR (CDCl_3) of *trans*-**9** at 298 K.

Spectra of *Rel*-(3*R*,4*S*)-4-(Aminomethyl)-2-hexyl-3-(pyridin-2-yl)-3,4-dihydroisoquinolin-1(2*H*)-one (*trans*-**10**)

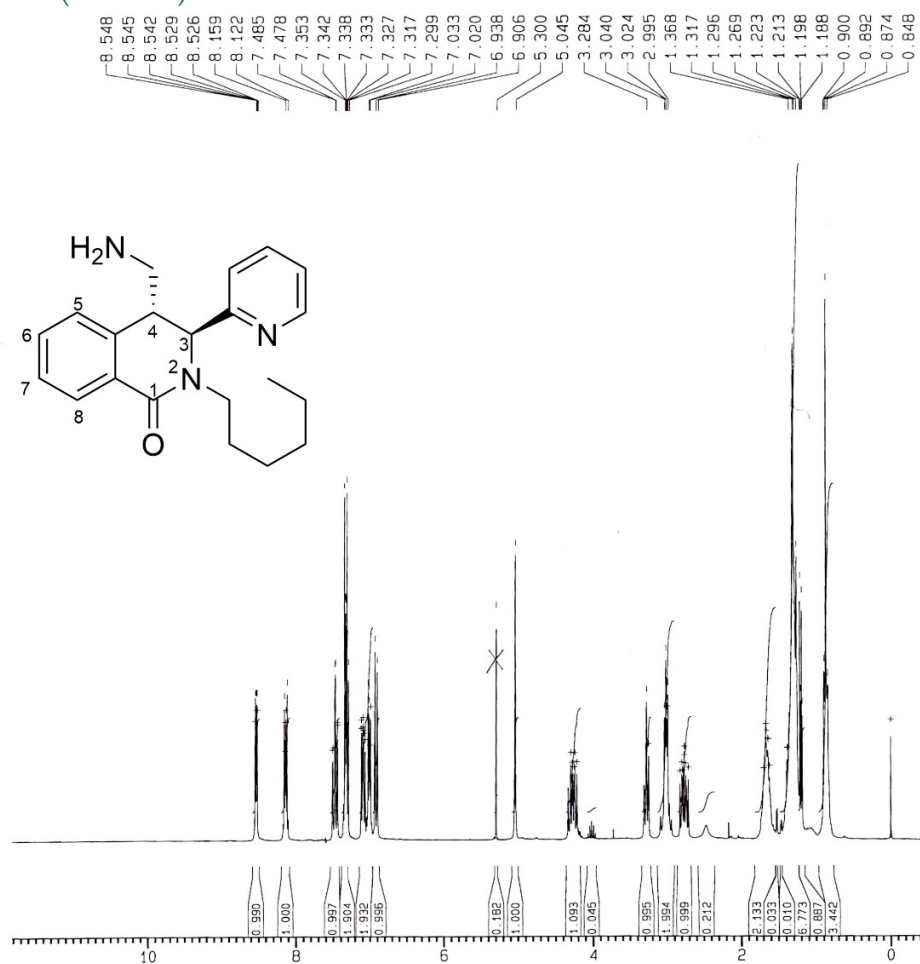


Figure S32. ^1H NMR (250.13 MHz, CDCl_3) of *trans*-**10** at 298 K.

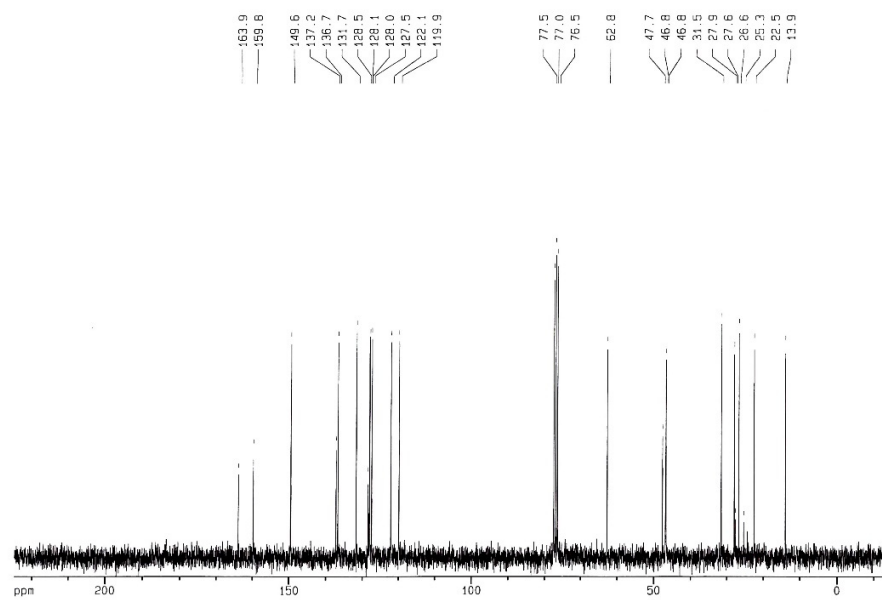


Figure S33. ^{13}C NMR (CDCl_3) of *trans*-**10** at 298 K.

Spectra of (*S*)-*N*-((3*R*,4*S*)-2-hexyl-1-oxo-3-(pyridin-2-yl)-1,2,3,4-tetrahydroisoquinolin-4-yl)methyl)-3-phenyl-2-(2,2,2-trifluoroacetamido)propanamide and (*S*)-*N*-((3*S*,4*R*)-2-hexyl-1-oxo-3-(pyridin-2-yl)-1,2,3,4-tetrahydroisoquinolin-4-yl)methyl)-3-phenyl-2-(2,2,2-trifluoroacetamido)propanamide (*trans*-**11a**+*trans*-**11b**)

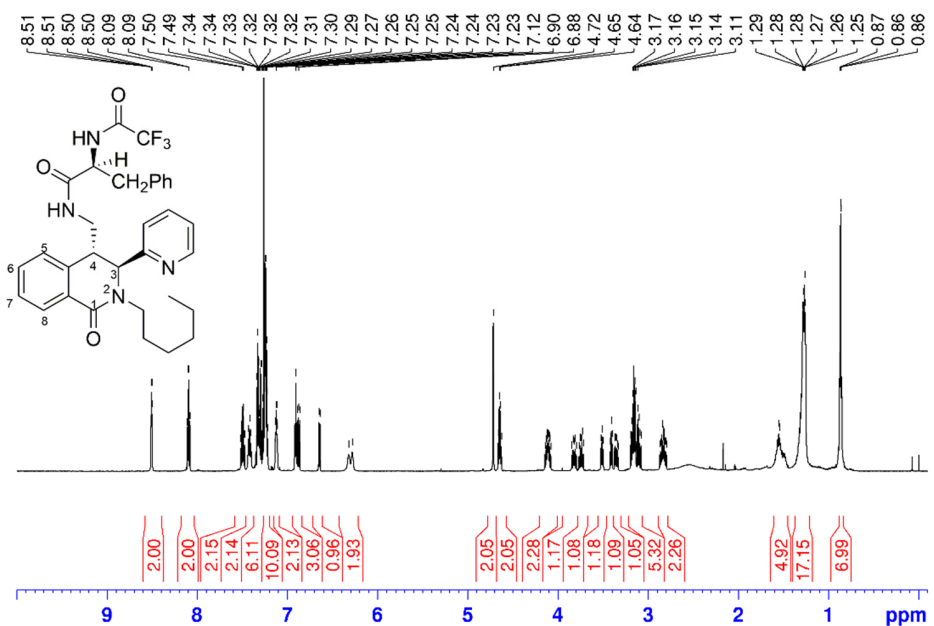


Figure S34. ^1H NMR (600.18 MHz, CDCl_3) of *trans*-**11a**+*trans*-**11b** at 298 K.

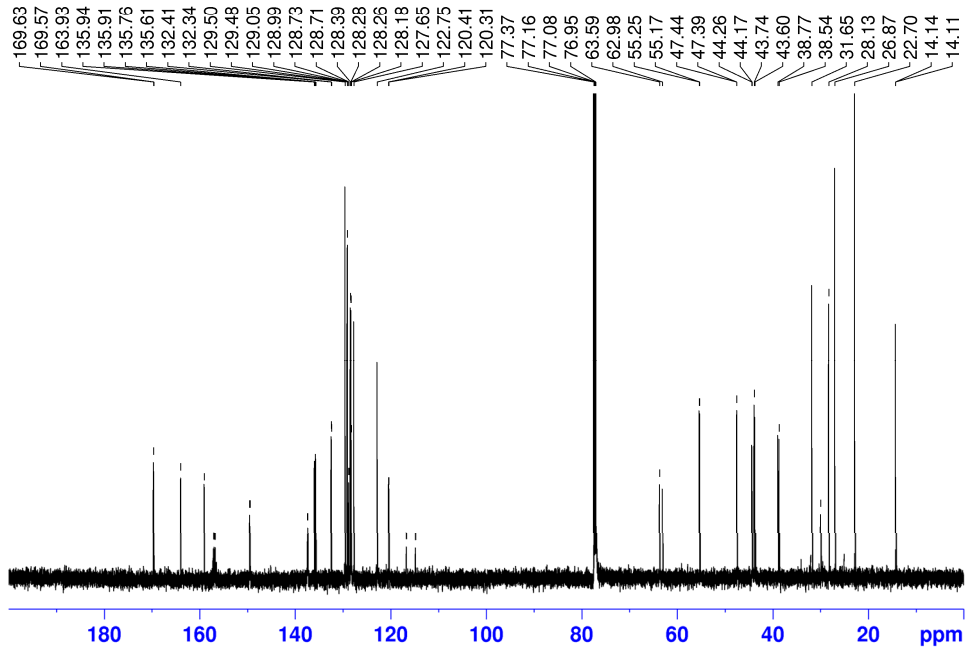


Figure S35. ^{13}C NMR (CDCl_3) of *trans*-**11a**+*trans*-**11b** at 298 K.

Spectra of *Tert*-Butyl (*S*)-2-(((3*R*,4*S*)-2-hexyl-1-oxo-3-(pyridin-2-yl)-1,2,3,4-tetrahydroisoquinolin-4-yl)methyl)carbamoyl)pyrrolidine-1-carboxylate and *tert*-butyl (*S*)-2-((3*S*,4*R*)-2-hexyl-1-oxo-3-(pyridin-2-yl)-1,2,3,4-tetrahydroisoquinolin-4-yl)methyl)carbamoyl)pyrrolidine-1-carboxylate (*trans*-**12a**+*trans*-**12b**)

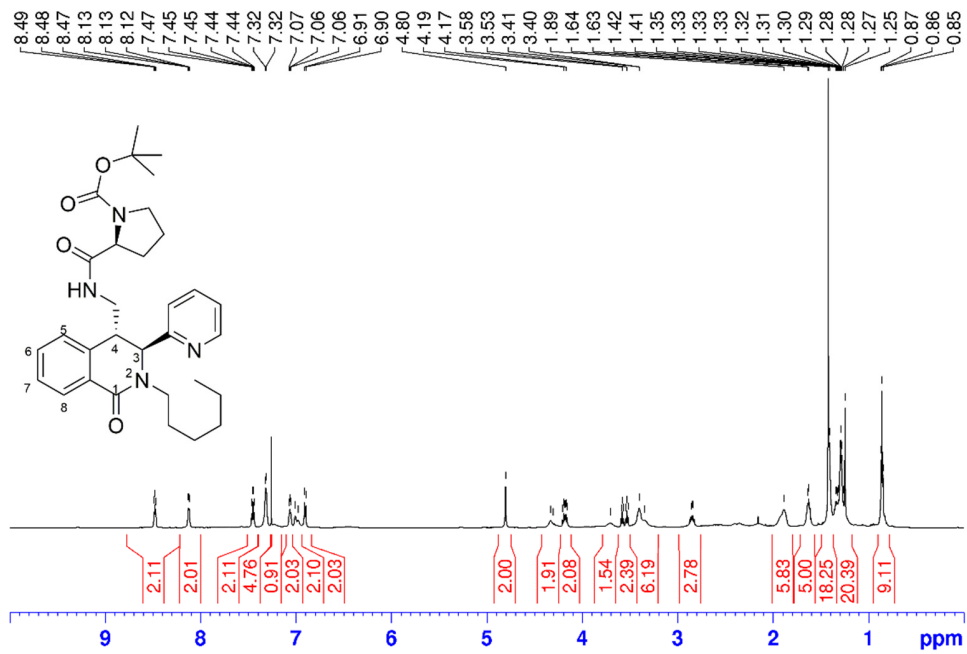


Figure S36. ^1H NMR (250.13 MHz, CDCl_3) of *trans*-**12a**+*trans*-**12b** at 298 K.

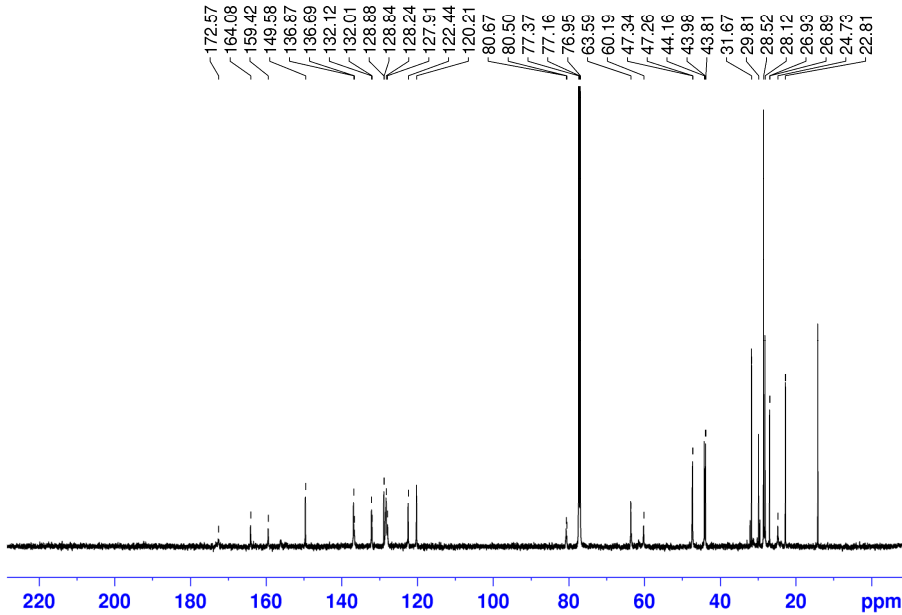


Figure S37. ^{13}C NMR (CDCl_3) of *trans*-**12a**+*trans*-**12b** at 298 K.

*(S)-N-(((3*R*,4*S*)-2-hexyl-1-oxo-3-(pyridin-2-yl)-1,2,3,4-tetrahydroisoquinolin-4-yl)methyl)-4-(methylthio)-2-(2,2,2-trifluoroacetamido)butanamide and (S)-N-(((3*S*,4*R*)-2-hexyl-1-oxo-3-(pyridin-2-yl)-1,2,3,4-tetrahydroisoquinolin-4-yl)methyl)-4-(methylthio)-2-(2,2,2-trifluoroacetamido)butanamide (*trans*-**13a+trans**-**13b**)*

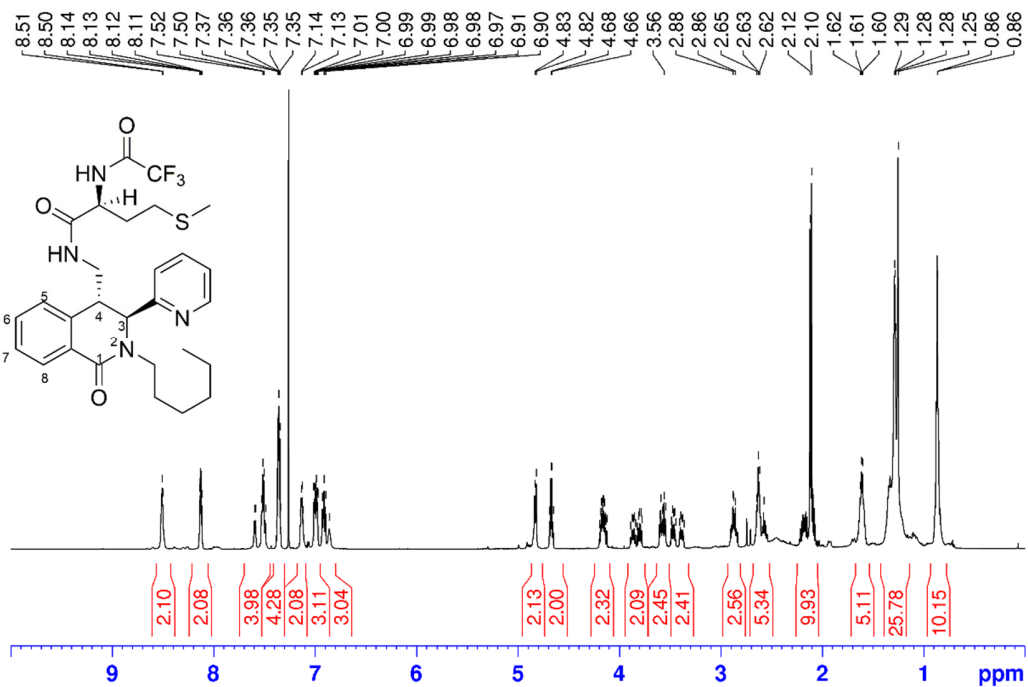


Figure S38. ^1H NMR (250.13 MHz, CDCl_3) of *trans*-**13a+trans**-**13b** at 298 K.

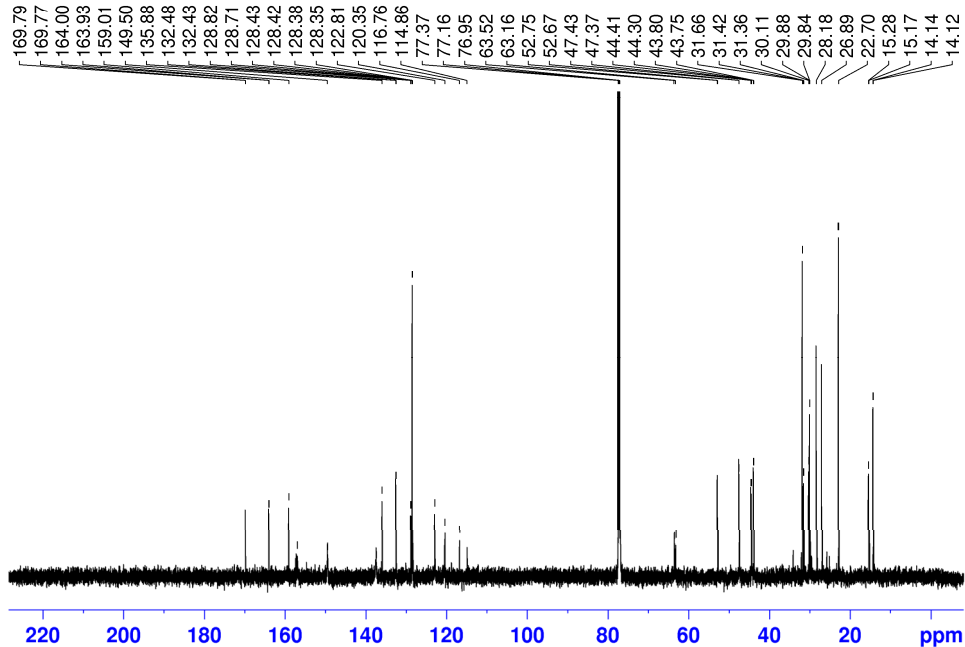


Figure S39. ^{13}C NMR (CDCl_3) of *trans*-**13a+trans**-**13b** at 298 K.

Optimized geometry at PCM/M06-2X/6-31+G(d,p) level of theory (solvent dichloroethane) of trans-6a'

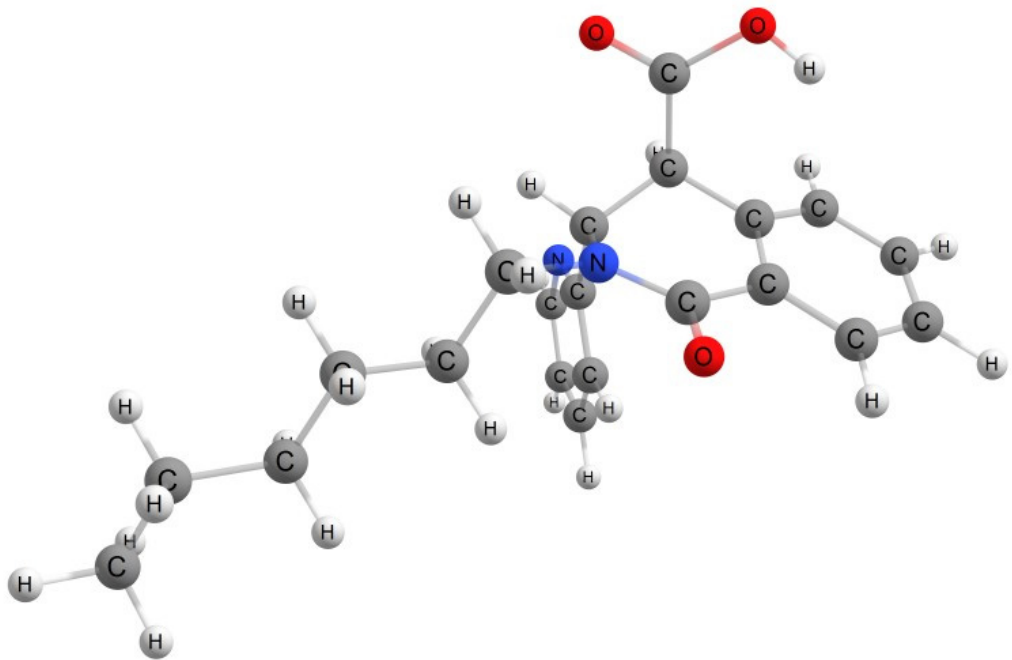


Figure S40. Optimized geometry at PCM/M06-2X/6-31+G(d,p) level of theory (solvent dichloroethane) of trans-6a'